COLLEGE OF SOCIAL SCIENCE

DEPARTMENT OF GEOGRAPHY AND ENVVIROMENTAL STUDIES

THE SPATIO TEMPORAL RELATIONSHIP BETWEEN LAND USE LAND COVER CHANGEANDLAND SURFACE TEMPERATURE CHANGETHE CASE OF HAWASSAAREA,ETHIOPIA

A Thesis Submitted to the Department of Geography and Environmental Studies in Partial Fulfilment of the Requirements for the Degree of Master of Arts in Geography and Environmental Studies (Specialization in GIS, Remote Sensing, and Digital Cartography)

By: ALIY YIMER

ID: GSR/7551/15

Advisor:Mr. Mola Maru

June, 2024

Addis Ababa, Ethiopia

THE SPATIO TEMPORAL RELATIONSHIP BETWEEN LAND USE LAND COVER CHANGE AND LAND SURFACE TEMPERATURE CHANGE THE CASE OF HAWASSA AREA, ETHIOPIA

A thesis submitted to the department of geography and environmental studies in partial fulfillment of the requirements for the degree master of art in GIS, Remote sensing, and Digital Cartography.

June, 2024

Addis Ababa, Ethiopia

Addis Ababa University

Collage of Social Science

This is to certify the thesis prepared by Aliy Yimer Yesuf entitled as **ASSESSING THE SPATIO TEMPORAL RELATIONSHEP BETWEEN LAND USE LAND COVERCHANGE AND LAND SURFACE TEMPRATURE CHANGE IN HAWASSA AREA, ETHIOPIA**. Using geospatial tools is submitted in partial fulfilment of the requirements for the Degree of the Masters of Art in Geographic Information System, Remote Sensing, and Digital cartography complies with the regulation of the university and meets the accepted standard with respect to originality and quality.

Signed by the Examining Committee:

Mr. Mola Maru		
Advisor	Signature_____	Date___/___/_____
Dr. AsmamawlL.		
Chairman	Signature_____	Date___/___/_____
Dr. AsmamawlL.		
Internal Examiner	Signature_____	Date___/___/_____
Dr. Shimeles Damene		
External Examiner	Signature_____	Date___/___/_____
Head	Signature_____	Date ___/___/_____

Acknowledgments

Frist and for most I would want to express my gratitude to "Almighty Allah," who made it possible for me to successfully finish my studies in the allotted short amount of time. He also gave me the patience and strength to do so. Other than "God," a great deal of individuals and institutions deserve our sincere gratitude for their invaluable contributions to this research.

I would like to sincerely thank my adviser, Mr. Mola Maru, for his assistance and support throughout this study. He assisted me from the outset of the research until its compilation, spending their time with me for insightful talks.

I would also like to express my gratitude to Ethiopian Space Science and Geospatial Institute, my workplace, for enabling me to pursue my MA degree. Additionally, I would like to express my gratitude to the Ethiopian National Meteorological Authority (ENMA) for giving me access to free climate data.

I would especially like to thank my classmates and my family for their unwavering support and gratitude. In closing, I would want to express my gratitude to everyone who has ever been my teacher, friend, or helper in the beginning of this arduous road. Too many to mention here, but a lot of them motivated me to grow and study.

Contents

List of Tables

List of Figures

List of Acronyms

AVHRR	Advanced Very High-Resolution Radiometer
CSA	Central Statistic Authority
DEM	Digital elevation Model
ESA	European Space Agency
ETM+	Enhanced Thematic Mapper Plus
FAO	Food and Agriculture Organization
GIS	Geographic Information System
LST	Land Surface Temperature
LU/LC	Land Use Land Cover
MODIS	moderate resolution Imaging Spectroradiometer
MSI	Multi Spectral Instrument
NDBI	Normalized Difference Built up Index
NDVI	Normalized Difference Vegetation Index
NMA	Ethiopian Meteorological Agency
SVM	Support Vector Machine
TIR	Thermal Infrared
TIRS	Thermal Infrared Sensor
TM	Thematic Mapper
UHI	Urban Heat Island
USGS	United States Geological Survey
GLAD ARD	Global Land Analysis and Discovery Analysis Ready Data
NASA	National Aeronautics and Space Administration
SWIR	Short Wave Infrared

Abstract

The Hawassa area in Ethiopia is a crucial region for controlling the local climate, but it is also environmentally sensitive and vulnerable to the effects of climate change. Over the past few

decades, rapid social and economic growth has led to significant changes in land use and land cover in this area. However, the current impact of these changes on the variability of the local climate, particularly in light of climate change, is still largely unknown. Land cover analysis was performed using the multispectral bands from Landsat 5 TM, 7ETM+ and Sentinel-2A MSI.The normalized difference vegetation index was calculated from the near-infrared and red spectral bands. The normalized difference built up index was calculated from the short-wave infrared and near infrared spectral bands. Zonal and correlation statistics were calculated for the normalized difference vegetation index, normalized difference built up index andland surface temperature data. To investigate,land surface temperature, data from thermal bands of Landsat 5, 7, and 8 for the years 1988, 2008, and 2023 respectively. The findings clearly demonstrate that different types of surfaces have a significant impact on land surface temperature. There is a considerable variation in land surface temperature among various land useland cover types. Cropland, settlement (built-up land), and grassland all exhibit higher land surface temperature, while forested areas, water bodies, and agroforestry show lower land surface temperature. Water bodies and vegetation cover play a crucial role in regulating land surface temperature and mitigating the heat effects on the earth. The study also reveals a strong negative correlation between normalized difference vegetation index and land surface temperature (coefficient of determination (R2) = 0.9332 in 1988, 0.9288 in 2008, and 0.9431 in 2023). On the other hand, the coefficient of determination (R2) = 0.9908 in 1988, 0.995 in 2008, and 0.9771 in 2023clearly show a strong positive relationship between the Normalized Difference Built-up Index and Land Surface Temperature. Land cover change has become a vital aspect of current resource management and environmental change monitoring strategies. As a result, it is crucial for governmental and non-governmental agencies to prioritize both proper land use management and the ecological impact of each land cover. This is supported by the thesis results for example the trained of water bodies continuously decrease the all over the study year.

Keywords: NDVI, LST, Hawassa area, NDB, and LU/LC

CHAPTER ONE

1. INTRODUCTION

1.1. Background of the study

Land is a valuable asset for both economic activities and environmental processes. It is where we find environmental resources and economic assets. However, land is limited and faces growing pressure as human needs continue to increase.

The concepts of land cover and land use are two fundamental aspects of land that are distinct but interconnected(United Nations Statistics Division, 2019).The term "land cover" refers to the physical attributes of the Earth's surface, including soil, water, plants, and other natural features. On the other hand, "land use" refers to how people utilize the land for different purposes, such as agriculture, residential areas, and industries. Although land use is mostly influenced by land cover, these terms are closely linked and can be used interchangeably. For instance, land cover includes settlements, but by examining the structures and activities within them, we can determine whether the land is being used for residential or industrial purposes(Chaudhary et al., 2008).

Modern methods for monitoring and assessing ecological changes now give priority to monitoring changes in land use and land cover. The ability to view Earth from space has become essential in understanding human activities and their impact on natural resources over time. Observations from satellites provide unbiased evidence of rapid and often unrecorded changes in land use. In recent years, satellite data has become indispensable for organizing global resources and infrastructure, managing natural resources, and addressing ecological changes(Zubair, 2006).

Most clear result of human change of vegetative locales to develop is cultivated by metropolitan development. This is generally connected with populace development, changes in land use, region extension, and a few human-induced exercises(Halder et al., 2021).By projection, there will be more than 70% increment in the quantity of metropolitan occupants by 2050 because of the current development rate in urbanization(Huang et al., 2019).

Most of human actions are the essential driver of the consistent reduction in the amount of vegetation on the world's surface (Sahana et al., 2016). The decline in vegetation was a

facilitating element to the escalationin land surface temperature (LST). According to Z. Song et al., (2021)features that vegetation is the primary impacting ingredients that determined LST.The LST is one of the urgent signs of natural habitat of the climate. According toPhan et al., (2018), the LST is demonstrates the thermal condition of the Earth's skin, which is a significant part in local and worldwide land surface handling studies.

Lately, remote detecting has arisen as one of the most engaged philosophies for deciding these affectation, permitting investigations of huge metropolitan areas of LST, Metropolitan Problem areas urban hotspots(UHS) and land use and land cover (LU/LC) to be completed (J. Song et al., 2018). The investigation of the connection between the LST and LU/LC are fundamental to comprehend the impacts created by varieties in cover on temperature expands(Hidalgo-García & Arco-Díaz, 2022). In this way, examining and distinguishing the connections referenced above to moderate these progressions in the metropolitan climate becomes basic for keeping up with the climatic equilibrium inside a city.

LST is a significant marker for assessing the provincial habitat, particularly in enormous urban areas where the peculiarity of surface urban heat island (UHI) is extremely clear (Azad O. Rasul, 2016).It is generally subject to the warm attributes of various ground covers, like warm Capability and warm penetrability(Abir & Saha, 2021). In this way, LST is a mark of surface energy balance, showing a serious level of spatial fluctuation.

Geospatial technologies, such as GIS and remote sensing, are increasingly offering new instruments for sophisticated environmental management.A comprehensive analysis of the earth system, patterns, and changes from small to global scales across time are made easier by satellite data. This study has tried to quantify the current and past state of LU/LC and LST examine and chart their spatiotemporal relationship, assess the effect LU/LC on LST Hawassa area.

1.2. Statement of the problem

Rapid urbanization, deforestation, agricultural expansion, and other LU/LC changes significantly impact local and regional climates. These alterations influence the LST, creating complex spatiotemporal dynamics that affect ecosystems, biodiversity, and human livelihoods. Despite extensive research, there is still a gap in understanding the intricate relationship between LU/LC changes and LST variations, particularly in regions undergoing rapid development. This study

aims to investigate the Spatiotemporal relationship between LU/LC changes and LST changes over the past few decades, providing insights into how different land cover types contribute to thermal dynamics and identifying critical areas for sustainable land management practices. Through this research, we seek to inform policymakers and stakeholders about the implications of LU/LC changes on climate regulation and contribute to the development of strategies to mitigate adverse environmental impacts.

Both urban and rural temperatures are rising, and this trend is getting worse all the time. The ecosystem on Earth is a complex system made up of many interdependent elements that are always changing. These elements include biological, chemical, physical, and human influences(Emilio, 2008). The main drivers of Earth's shifting land use and cover patterns are industrialization, population expansion, and a variety of human and natural processes. The elements that contribute to the growing LST a result of changes in land cover and use. The environment is getting hotter because of changes associated to overgrazing, deforestation, haphazard settlement growth, and other human-caused activities.

This work is important because it has many real-world applications that offer useful data on LST and LU/LC conditions.This research aims to address the missing research gap regarding the impact of land use/cover dynamics on LST within the study area. Planning and decision-making procedures can be made more efficiently with the help of this information. According to Aires et al., (2001), land surface processes depend heavily on LST. In addition to controlling upward terrestrial radiation and acting as a climate change indicator, it also controls the exchange of sensible and latent heat flux between the surface and the atmosphere.

Occasionally, the Hawassa area experiences significant radiation on the biophysical surface material. Numerous ecological, social, and economic issues arise from the loss of forests, such as the extinction of biotic groups, a decline in biodiversity, soil erosion, global warming, and a reduction in the income of forest dwellers(Woldegebriel Tessema & Girma Abebe, 2023). In our country, some studies have been conducted onLST, especially in the rift area of the country. However, almost all of these studies have utilized coarse satellite imagery (Landsat) images and traditional classification methods. My study, on the other hand, employs Landsat and Sentinel(fine resolution)imagery.

The main justification for conducting this research project in the Hawassa area of Sidama Regional State is that:

- The regions are distinguished by a variety of plant life.
- Variable climate patterns
- Various topographic configurations
- Generally speaking, different LU/LC types and faster changes.

A key component of land management and planning plans that must concentrate on LST mitigation and the area's adaptation to the difficulties of climate change is an understanding of the influence of LU/LC change on LST(Getahun & Yoseph, 2022).

1.3. Objective of the study

1.3.1. General objective

This mastersof thesis main objective is toevaluate the spatiotemporalrelationshipbetween land use land cover changeand land surface temperature change in Hawassa area.

1.3.2. Specific objective

Two particular objectives were defined in order to attain the overall goal. These are the following:

- to analyze the temporal and spatial variation in LST in connection with LU/LC in the study area
- To estimate the magnitude of the effect on LU/LC changes (LU/LCC) on LST changes at different time periods.

1.4. Research questions

The following research questions should be the basis for all the actions that have to be determined by the overall and particular goalsmentioned above:

- What is the research area's spatiotemporal pattern of LU/LC change?
- What is the study area's primary LU/LC class?
- What function does NDVI serve in LST?
- What is the relationship in the research area between LU/LC and LST?
- What is the relationship in the research area between NDBI and LST?

1.5. Significance of the study

Environmental changes are a result of LU/LC alterations. The increased need for land for habitation, agriculture, and other human activity interventions is the cause of extensive LU/LCC. To reduce the impact of environmental changes on fluctuations in LST in Hawassa area, Sidama region, the following important usefulnesshave guided toconduct thisstudy:

- Environmental Impact. It is essential to comprehend the LU/LCC on LST in order to evaluate the environmental effects of human activity. This research will advance our knowledge of how variations in land cover and use impact regional temperature patterns.
- Urban Planning and Land Management.The practical repercussions(result) of the study's findings will be felt by land managers and urban planners. It will be possible to get important insights for developing sustainable cities, maximizing land use strategies, and reducing the urban heat island effect by mapping the effects of LU/LCC on LST change.
- Climate Change Adaptation and Mitigation.The dynamics of climate change are significantly influenced by LU/LCC. This study will aid in the development of mitigation and adaptation plans for climate change by evaluating the effects of LU/LCC on LST change.
- Policy Development.The results of the study can be used to guide the creation of policies for sustainable development, land management, and conservation. The findings can be used by governments and legislators to create more sensible land use regulations, give conservation initiatives top priority, and encourage sustainable land management techniques.
- Data-Driven Decision Making.The impacts of LU/LCC on LST change will be visualized through the use of mapping techniques and geographical analysis in this study. The maps and spatial patterns that are produced can give academics, stakeholders, and policymakers easily accessible information for making evidence-based decisions.
- Scientific Knowledge and Methodological Advancement.The present investigation aims to enhance our comprehension of the intricate interplay of temperature dynamics, land use, and land cover, thereby augmenting the body of scientific knowledge.

1.6. Scope of the Study

The investigation took place in the Hawassa area of Ethiopia's Sidama Region. The land-use and land-cover patterns in this area differ and have undergone periodic changes. Consequently, there have been occasional increases in the LST in the Hawassa area. The objective of this study was to calculate the trend of LU/LC change, establish the relationship between LU/LC and LST, and assess how LU/LC dynamics impact changes in LST. LST readings were evaluated and the classification of LU/LC was validated using Google Earth for all land use and land cover categories.Seasonal fluctuations and climate change are two environmental problems that result from increasing LST. Failure to appropriately manage agricultural and settlement land can have a negative impact on the ecology.

1.7. Limitation of the study

This study attempted to gather all the data required for processing, interpretation, and analysis. Nevertheless, there have been certain limitations to this thesis study. Getting data from various governmental organizations was too bureaucratic and troublesome. Another limitation is that, for various reasons, the impact of altitude on LST was not studied. Additionally, due to security reasons, the researchers were unable to collect enough ground control points for verification purpose.

1.8. Structure of the thesis

There are six chapters in this thesis. The back ground of the study, problem statement, objectives, significance, scope, and limits are all included in the first chapters. The literature review is covered in detail in the second chapter, with particular emphasis on ideas related to land cover change and its effects, NDVI, and LST and its algorithms in general.The data required for the study and the procedures used to extract conclusions from the input data are described in Chapter 3.The main land cover types and their changes, the NDVI and LST's temporal and spatial distribution, and the impact of land cover change on LST distribution are all covered in the fourth chapter. This chapter also presents the association between NDVI, NDBI, and LST as well as the relationship between land cover with NDVI and land cover with LST.The discussion portion is covered in Chapter 5, and the findings and suggestions are covered in Chapter 6. Important discoveries and issues that require more research have been included in this section as recommendations for decision makers.

CHAPTERTWO

2. LITERATURE REVIEW

2.1. Basic concepts of land use land cover changes (LU/LC)

Earth's biodiversity has been negatively impacted by the swift growth of agriculture and human settlements, which has also simplified natural ecosystems. If land resources continued to be threatened and overextended, the integrity of ecosystem products and services would be in peril(Elias et al., 2019).Due to its substantial impact on climate change worldwide, LU/LC shifts have thus become a major environmental research community issue in recent years (Elias et al., 2019).The greatest threat to the global depletion of natural resources particularly wetlands, forests, and a variety of wildlife is LU/LC, which also plays a role in global environmental change(Belete et al., 2023). One of the main causes of environmental deterioration is the conversion of forest cover to other land uses in order to satisfy human needs and desires(Gebrelibanos & Assen, 2015). Destroying habitats and creating ecological imbalances on Earth's surface(FAO, 2020).According to (Belete et al., 2023), due to their capacity to produce food, medicine, precipitation, and other necessities for thousands of people, forests are important components of biodiversity and a major source of income, (FAO, 2016).Clean water and a place to store carbon, which lessens the consequences of climate change worldwide.

Theterrestrial environment, which includes the surface's biological and physical components, encompassing man-made surfaces, agricultural regions, forests, (semi-)natural areas, marshes, and water bodies, is referred to as land cover (biophysical properties of the earth's surface).The word "land use"refers to the socio-economic function or current and anticipated functional dimension (e.g. residential, industrial, commercial, agricultural, forestry, recreational) of a region. On both a regional and temporal scale, LU/LC alteration is increasingly acknowledged as a significant contributor to environmental deterioration and quality loss. Changes in LU/LC have a major influence on declining forest cover and biodiversity decline, and climate change.Furthermore, one of the elements affecting runoff, soil loss, and stream flow is LU/LC change(Woldeamlak, 2002). As LU/LC change rises, it is important to integrate data from Earth observation with human experience to develop a thorough understanding of the patterns, causes,

and effects of these changes(Grinblat et al., 2015).It's critical to comprehend how the community views the causes and effects of LU/LC shifts in order to put policies in place to reduce them.

2.2. Factorsfor land-use and land-cover changes

Wilderness areas, or unspoiled places, are thought to make up roughly 46% of the planet's land area. Roughly 50% of Earth's area was covered by forests eight thousand years ago; today, that percentage is only about 30%. Worldwide, agriculture has invaded forests, savannas, and steppes to meet the expanding demand for food and fiber. Multiple sources of data, including the Global Forest Resources Assessment 2000, demonstratethat throughout the 1990s, the world's naturalforests lost an average of 16.1 million hectares annually, resulting in a 4.2% decrease in the coverage of natural forests since 1990(Lambin et al., 2003).

There is a complicated and dynamic link between changes in land use and cover and the variables that give rise to them. Both socioeconomic and natural elements influence it. According to some research, demographic dynamics influence changes in land cover more than any other factor(Mather & Needle, 2000). Some argue that the primary contributing element is the dominance of economic concerns(Lambin et al., 2001). Land cover change is influenced by a number of socioeconomic factors, such as the availability of financing and markets, tenure instability, and destitution D. J. Campbell et al., (2005). These distinctions between and within certain nations and areas have come to light. Therefore, given the context of regional variances, the diversity of generating drivers of land use change must be considered(H. Geist et al., 2006).

Studies on LU/LC (for example, Ojima et al., 1994,1995;Lambin et al., 2001), demonstrated that the drivers behind changes in land use are socioeconomic and biophysical. Proximate causes and underlying causes are the two categories into which driving forces are typically separated. The actions and activities that have a direct impact on land use such as road construction or timber extraction are known as proximate causes. The "fundamental forces" that support the proximate causes are known as underlying causes, and they include institutional, cultural, technological, economic, and demographic aspects (H. J. Geist & Lambin, 2002).

2.3. Land-use and land-cover change in Ethiopia

Indeed,the rapid agricultural expansion and population growth may be responsible for the substantial changes in LULC observed worldwide (Tolessa et al., 2020).East Africa (The Horn of

Africa) is not an exception to these changes in land use and cover, just like the rest of the world (Berihun et al., 2019).Ethiopia has experienced particularly noticeable and swift changes as a result of population pressure, relocation initiatives, climate change, and other factors influenced by both nature and human activity. Similar to other nations, the main causes negatively affecting Ethiopia's landscape's natural state are human activity(Marchant et al., 2018), including negative and harmful effects on the environment and way of life(Tefera, 2011);(Gebreslassie, 2014).

One of the biggest environmental issues facing the globe now is the decline of forests (Mitchell et al., 2017);(Ranagalage et al., 2020). Forest resources are under increased pressure from agriculture in order to feed the world's rapidly expanding population(Deribew & Dalacho, 2019); (Negassa et al., 2020). The primary causes of deforestation in developing nations are the dispersal of cultivated land into forest land, the manufacturing of lumber and charcoal, and the harvesting of wood are the main factors of deforestation in third world countries(Muhati et al., 2018). Like other emerging nations, Ethiopia saw a sharp reduction in its forest cover as a result of settlements, overgrazing, and agricultural encroachment(Tesfahunegn, 2014). For example, the country's forest cover decreased from 35% at the beginning of the 20th century to 2.4% in 1992(Sayer et al., 1992). Through the implementation of an afforestation and re-afforestation program, the Ethiopian government has recently reported on the increasing trend of forest cover.The loss of topsoil due to erosion has risen as a result of the diminishing forest resources, potentially lowering agricultural yields and exposing agrarian people to food insecurity.

Because they absorb carbon dioxide and mitigate global warming, forests are essential to addressing climate change (Negassa et al., 2020). Despite forests' ability to mitigate the effects of climate change, between 1995 and 2016, Ethiopia lost over 141,000 hectares of forest annually (1.1%)2010(FAO, 2010).

2.4. Remote Sensing

The subject of remote sensing has grown interesting and glamorous in recent years, with opportunities growing quickly. Large sums of money are invested in these fields by many organizations. This raises the question of why these fields have become so significant recently. There are two primary causes for this:

- Nowadays, there is a growing interest among scientists, researchers, students, and even regular people to gain a deeper understanding of our surroundings. The physical location of their study area and the activities that occur there are referred to as the environment. Put another way, we've come to understand that geographic space and the information that describes it are a part of our daily lives and that nearly every choice we make is impacted or determined by a geographical truth.
- The increasing availability of sophisticated space technology and the decreasing cost of computer hardware and software to process large volumes of spatial data have made remote sensing accessible to a wider range of people and suitable for complex environmental spatial situations.

Remote sensing is the study of collecting information about the Earth's surface without having direct physical touch with it. To do this, energy that is reflected or emitted must be found, recorded, and processed. The data collected must then be used for analysis and application. The interaction between incident radiation and the targets of interest is a common phenomenon in remote sensing (Kumar, 2018).

The core of earth observation is the collecting of geospatial data. Information on the physical, chemical, biological, and geometrical characteristics of our planet is gathered through earth observation, which aids in the assessment of the state and monitoring of changes in the natural and cultural environments. Thus, earth observation is used for mapping, monitoring, and forecasting.Geospatial data is obtained through earth observation. The process of gathering geospatial data can be thought of as the first step in our development cycle, which also includes observation, analysis, designing or planning, building or developing, and so on(Tempfli et al., 2009).

2.5. Geographic Information System (GIS)

A geographic information system (GIS) is a specialized computer program that stores, manipulates, processes, and displays geographic data as maps. All GIS software vendors offer a database management system that handles and integrates both attribute data and spatial data. Spatial data refers to real-world geographic objects such as lakes, countries, buildings, and highways, along with their corresponding locations.These objects have additional characteristics, including names, number of stories, depth, or population. GIS software links spatial and attribute

data, enabling the development of information and facilitating streamlined analysis. This allows for simultaneous tracking and analysis of both the spatial and attribute data (J. Campbell & Shin, 2011).

Geographic data is converted into geographic information in a GIS. However, a complicated web of operations and procedures is involved in this seemingly simple change. In other words, raw positional feature data with attributes is the starting point for geographic data. Next, complementary and/or opposing data sets are superimposed over this data to create coincident correlations. After analysis and geo-processing, relationships and data are provided as geographic information products. These geographic information products are often interactive software tools intended to aid in decision-making(Galati, 2006).

Geographic data are frequently modeled in a space called vector space. All that a vector space is a platform for geographic vector data, which represent Earth features using x-y coordinates together with lines and shapes. Non-topological coordinate geometry and attribute information for spatial features are stored in geographic vector data. Raster data is another important category of geospatial data. Raster data are digital images that are shown as a grid of cells, or valued pixels. The characteristics and looks of these depend on the kind of image and the quantity of colors depicted (Galati, 2006).

2.6. Role of Remote Sensing and GIS in Land-use and Land-cover change

Technology development has made it possible to provide and combine data from remote sensing with other types of data to help produce informative content.Global Land Analysis and DiscoveryAnalysis Ready Data (GLAD ARD) tool, an application that facilitates the provision of globally consistent ARD for earth observation, is one initiative that further enhances this. Another is the automated Landsat data processing system(Potapov et al., 2020). Since remote sensing allows for observations across bigger areas of the Earth's surface than are achievable with ground-based observations, it is a crucial instrument in the field of land change science.To do this, RADAR, LiDAR, cameras, and multispectral scanners installed on air- and space-borne platforms are used.Aerial photographs, satellite imagery, and RADAR and LiDAR databases are the outcomes.Effective policy planning and implementation are facilitated by the ability to depict data on resources that are both naturally occurring and intentionally manufactured in spatial domains thanks to GIS(Roy & Roy, 2010).GIS and remote sensing technologies were used to

map the spatial distribution of land resources together with their proper status and present threats using multispectral and multi-temporal Landsat photographs(Moisa et al., 2023).

Studying and tracking changes in land use and cover requires the use of remote sensing and GIS. They offer useful methods and instruments for gathering, examining, and displaying geographical data pertaining to the dynamics of land use and cover.Obtaining Data Drones, satellites, and aircraft sensors are examples of remote sensing technology that can gather data and imagery across vast distances (Mariye et al., 2024). Comprehensive data on land-cover types, vegetation density, urbanization, deforestation, and other changes in land-use are available from these data sources. These many datasets can be managed and integrated with the aid of GIS. Organizing and Charting Types of land cover can be mapped and classified using remote sensing data, especially high-resolution satellite images. Classification algorithms, either supervised or unsupervised, can be used to distinguish and classify various land-use types using satellite imagery(Mariye et al., 2024).

To identify changes in land use and land cover, remote sensing technologies are employed in a variety of ways. While some research have merged remotely sensed data with GIS data, others have actually used remote sensing techniquese.g. (Rogan & Miller, 2006).

It has been demonstrated that remote sensing and GIS technology may produce results and policy recommendations that are supported by science. This has helped planners and decision-makers promote sustainable development, particularly in rapidly expanding urban areas(Addo, 2010).Remote sensing and GIS have been extensively utilized approaches to better understand the spatiotemporal and spectral elements of changes in land use and cover at local and global scales (Rogan & Chen, 2004; Weng, 2010).The fundamental component of these methods is the examination of geographic modeling(Rogan & Chen, 2004; Coppin et al., 2004).Seeks to identify the locations of any changes that have occurred or may occur(Veldkamp & Lambin, 2001). The majority of these models evaluate historical land use data in order to forecast future land use scenarios by combining environmental variables with the assessment of past land transformation and transition(Eastman, 2009).

2.7. Land Surface temperature

LST is the thermodynamic temperature of a thin layer at the interface between the atmosphere and the soil, plants, or other surface elements.In order to recover LST from satellite Thermal Infrared (TIR) data, a number of parameters must be measured. These comprise the following: integrating the impacts of viewing geometry and fraction of cover vegetation; quantifying spatial variability across land cover; surface emissivity correction; and atmospheric and radiometric calibrations. These factors depend on the atmosphere's condition as well as the emissivity of the materials on the land(Sattari & Hashim, 2014).

Satellite LST products provide an approximation of the earth's surface kinetic temperature(Becker & Zhao-Liang Li, 1995),that is, the mass surface instrument as seen by the sensor down to around 12 μm in depth.The average effective radiative heat of different soil and canopy surfaces is often estimated using the earth's surface thermal emission to determine skin temperature(Hall et al., 1992;Betts et al., 1996).LST is an important parameter in land surface processes and a helpful indication of climate change because it controls upward terrestrial radiation, which controls the interchange of surface sensible and latent heat flux with the atmosphere(Aires et al., 2001;D. Sun & Pinker, 2003).For instance, the difference in skin temperature and surface air temperature primarily regulates energy exchanges along the land-surface boundary, which

impacts, despite their close proximity, how the surface and air respond to outside stimuli on distinct temporal and geographical scales(Y. Sun, 2008).Satellite-focused One can use thermal emission at microwave or infrared atmospheric windows wavelengths to determine the temperature of the terrestrial surface. Although brightness is directly captured by onboard sensors, the derivation of LST from it is questionable,(Y. Sun, 2008).TIRbased LST retrievals are less uncertain (1-2K) than microwave-based ones because surface emissivity ranges are shorter and brightness is more temperature-dependent in the TIR domain(The Scientific Committee, 2008).

2.8. Urban heat island

The phenomena where cities have greater temperatures than the surrounding rural areas is knownasurban heat island. The concentration of man-made features like roads, buildings, and

infrastructurewhich both absorb and reemit solar heat more than natural environments like woods and water bodiesis the primary source of urban heat islands.The lack of flora in metropolitan areas also adds to the increased heat. Urban regions can be up to 17°F hotter during the day than rural locations, while the difference in temperature at night can be as much as 2–5°F higher(Vujovic et al., 2021)

When air temperatures (AT) rise in cities relative to their rural counterparts, it is documented that an urban heat island (UHI) has occurred. The UHI phenomenon arises when cities replace the natural land cover with densely packed areas of heat-absorbing buildings, pavements, and other surfaces.It's a kind of air pollution that fuels global warming as well. In contrast to the nearby suburban and rural areas. The temperature of urban regions, such city centers, is elevated by UHI(Stewart & Oke, 2012).

The primary variables employed in UHI research are air temperatures and LST,this is derived from data from thermal infrared remote sensing.The term "UHI traditional weather station automatic temperature measurements" refers to the distinction between the AT within the city and the AT of its surroundings(Tzavali et al., 2015)the two main methods for analyzing the UHI phenomena are LST measurements or TIR remote sensing data.

primarily three kinds Based on several layers of the urban atmosphere and surface characteristics, UHI can be classified as canopy layer heat islands (CLHI), boundary layer heat islands (BLHI), and surface urban heat islands (SUHI) (Voogt & Oke, 2003;Yuan & Bauer, 2007).The majority of surfaces in cities have a high heat capacity. While SUHI, also known as land surface temperature, reflected the surface thermal qualities, CLHI and BLHI are mostly linked to atmospheric heat islands(Yuan & Bauer, 2007).Because LST, which is influenced by the brightness and reflectance of the earth's surface, ultimately determines the efficiency of heat exchange between the earth and atmosphere, it may be used to effectively simulate climate change, build urban areas that are sensitive to climate change, and maintain regional and global energy balance(Chayapong & Dasananda, 2012)

Urban materials' thermal behavior is influenced by both thermodynamic or equilibrium state attributes (such as density and specific heat capacity) and thermal physical factors associated to energy movement across a system (such as radiation, conduction, and convection)(Georgakis &

Santamouris, 2017).The UHI benefits from those material attributes. The concrete structure's thermal equilibrium is dependent. The ability of materials to absorb and storeheat in addition to other thermal characteristics, thermal inertia affects heat. The quantity of heat that is released into space, convectional heat transfer to the air, thermal energy stored in material masses, absorbed and stored solar radiation, and heat conducted to the earth(Santamouris, 2013).

2.9. Effects of LU/LC on land surface temperature

As a result of LU/LC classes transformation to non-evaporating surfaces, the surface temperature has increased (Sahana et al., 2016).It is becoming increasingly crucial to fully examine how LU/LC modifications affect the overall rise in the LST. LU/LC surfaces and types have been examined to define LST because they emit and absorb energy radiation in different ways(Pongratz et al., 2010).Researchers have also improved from the estimation of the cross-sectional link between LST and LU/LC types when examining the effects of changing land cover on LST over time(L. Liu & Zhang, 2011).

The growing world population is driving up demand for housing, food, shelter, and agricultural output. Because of human activities, the land cover is shifting to make room for the expanding populationdemand and replace vegetated areas with impermeable surfaces, unconsciously contributing to climate change(Igun & Williams, 2018; Nzoiwu et al., 2017).

Through limiting nutrient loss, mitigating soil erosion, and preserving the hydrological cycle, vegetation ensures the ecosystem's survival. Changes in land cover have therefore emerged as one of the key markers of environmental vulnerability (Nzoiwu et al., 2017).Changes in land cover change the atmospheric concentration of carbon dioxide as well as the albedo, evapotranspiration, and surface irregularity of the land(Purwanto et al., 2016;Zhang & Liang, 2018).

The effects of land use and conversion on environmental decline can be quantified by changes in LST among various landscape features (F. Zhang et al., 2016).Due to the fact that every form of land cover has different radiation and absorption properties, there may be significant LST variances over the various LU/LC units and changes(Ahmed et al., 2013); (Debie et al., 2022);(Sinha et al., 2015).The land use cover pattern's symbol is reflected on LST as it changes(Pal & Ziaul, 2017).

The spatial distribution of land surface temperatures amid urban development is caused by changes in land use or cover(Zhao et al., 2017). Agricultural soils and aquatic bodies have lower surface temperatures than well-constructed land cover, which includes commercial buildings, industry, and walkways. Due to its tendency to act as a canopy and evapotranspiration, vegetation helps to counterbalance the effects of UHI and can even make an area feel colder than it does outside. Therefore, in order to lower high urban temperatures, it is advised to increase vegetation cover(Zhao et al., 2017).

2.10. Normalized Difference Vegetation Index

When utilizing remote sensing data, especially from satellites, to measure the health and density of vegetation, one popular metric is the NDVI. It is computed by measuring the difference between red light, which plant absorbs, and NIR light, which vegetation strongly reflects(Yengoh et al., 2014). (NIR - RED)/ (NIR + RED) is the formula used to calculate the normalized difference between the two reflectance: NIR stands for near-infrared reflectance, and RED for red reflectance. The NDVI scale has values between -1 and +1; lower values generally represent water or clouds, values near 0 represent bare soil or urbanized areas, and higher values positive values indicating dense green vegetation. NDVI is used to assess vegetation density, monitor changes in plant health, and understand vegetation patterns and dynamics(Rouse et al., 1974).The index finds extensive application in many fields such as land management, forestry, agriculture, and environmental monitoring. It supports the monitoring of ecosystem health, the detection of changes in vegetation conditions over time, the estimation of crop yields, and the assessment of the effects of drought and other environmental factors on vegetation.

In vegetative studies, NDVI has been widely applied; among other things, it has been used to assess crop yields, pasture performance, and rangeland carrying capacities. It frequently has a direct correlation with other ground characteristics like the percentage of ground cover, the plant's photosynthetic activity, surface water, the leaf area index, and the quantity of biomass(S D A P S A & NATIONAL REMOTE SENSING CENTRE, 2014).

In order to power photosynthesis, green leaves absorb solar radiation in the spectral region known as photo synthetically active radiation (Jensen, 2007). To be more precise, the green spectral region of leaves does not absorb solar energy as much as the blue and red spectral regions do.Green leaves are very reflective in the near-infrared spectrum and absorb no light,

(Jensen, 2007). Green leaves therefore have positive NDVI ratings due to their high near-infrared reflection and high absorption of visible light.

Water has a negative NDVI value, but bare soil, clouds, snow, and concrete have values that are almost equal to zero (Goward et al., 1985).The photo synthetically active radiation absorbed by plant canopies, photosynthetic capacity, net primary productivity, leaf area index (LAI), percentage of absorbed photo synthetically active radiation, carbon uptake, and evapotranspiration have all been shown to be strongly correlated with NDVI(Myneni et al., 1995, Buermann et al., 2002,Hicke et al., 2002). Hence, NDVI makes it possible to track the photosynthesis of vegetation over time and to make simple comparisons between different times and places(Myneni et al., 1997). It is useful for mapping, evaluating, or forecasting the incidence and consequences of disturbances including frost, fire, flood, and drought (Pettorelli et al., 2006), along with aiding in the mapping and forecasting of the degree of land degradation (Prince et al., 2009).

2.11. Conceptual Frame Work

A conceptual frame work is an illustration that helps illustrate the expect relationship between cause and effect in research. It lies up the pertinent goals for the investigation and shows how they connect to produce logical findings. When evaluating changes in land cover and use and analyses its correlation with LST. A conceptual frame work can be developed to understand the relationship between different variables. In this case the variable would include LU/LC types and their impact on LST.

The conceptual frame would consider various type of landscapes such as settlement, agroforestry, rocks, metal roads, concrete infrastructure, water bodies, wet lands, forests, grass lands, wood vegetation and crop land. These different types of land scape have varying effect on LST. E.g. Settlement and concrete infrastructure tend to enhance LST, while water body, wet lands, forest and woody vegetation tend to reduce LST. This land use structure coverage and state of health differ in different seasons, which are also conceded in the conceptual frame work. Understanding the connections between land uses, types of cover and LST allows for the examination of how LU/LC affects LST and their identification of any relationships.

Creating a theoreticalstructure to evaluate LU/LC and examining how they relate to LST requires researching previous studies in the field. This review helps identify relevant variables and their relationship, which can then be incorporated into the conceptual frame work. This conceptual framework provides a methodological approach to understanding the complex relationship between land use, cover change and LST. It serves us a guide for a research, helping to define research questions identify variables and analyses the expected cause and effect relationships.

CHAPTER THREE

3. MATERIAL AND METHODES

3.1. Description of the study area

3.1.1. Location

The study takes place in the Hawassa area of the Great Rift Valley. Geographically, the region covers an area of 1026.5 $km^2$and is situated between 6^0 48' 0" - 7^0 10' 0" N and 38^0 15' 30" - 38 ^{0}43'0" E (Fig.1). Located in the Great Ethiopian Rift Valley, the region sits at elevations ranging from 1571 to 2714 meters above sea level. It is located 273 km south of Addis Ababa, the capital city of Ethiopia. The area includes three districts, or werdas, and one city administration: Wondo Genet, Hawassa Zuria, Malga, and Hawassa City. This area was chosen for the study because it demonstrates how different ratios of land use to land cover represent a range of landscape diversity. Additionally, the area is known for its warm, humid to sub-humid tropical weather.

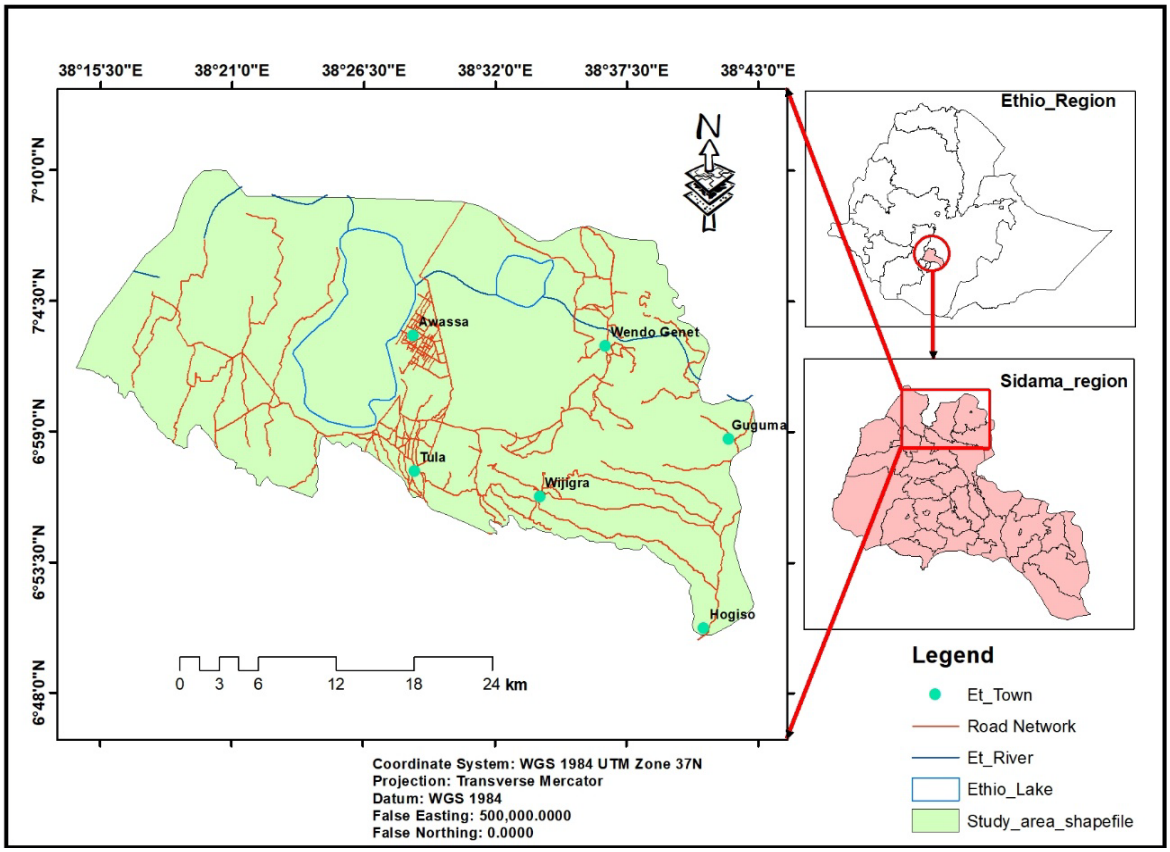

Figure 3.1. Location map of the stud area

3.1.2. Topography

Topography refers to the study of the earth's surface, including its shape, features, and related phenomena. In the Hawassa area, there are two prominent topographical features: the flat plains located at the base of the mountains, and the volcanic mountains that create the surrounding escarpments. The elevation of the research area is depicted in Figure.2a.

Based on the slope of the region, 98.5 km^2, or 95.86%, of the Hawassa area falls within the range of 0 to 24^0, while 40 km^2, or 3.89%, is found between 24^0 and 48^0. Additionally, 1 km^2, or 0.09%, is situated between 48^0 and 71^0. The slopes of 71^0 can be found in the eastern, northeastern, and southeast ridge section of the area. The slope of the area is depicted in Fig. 2b.

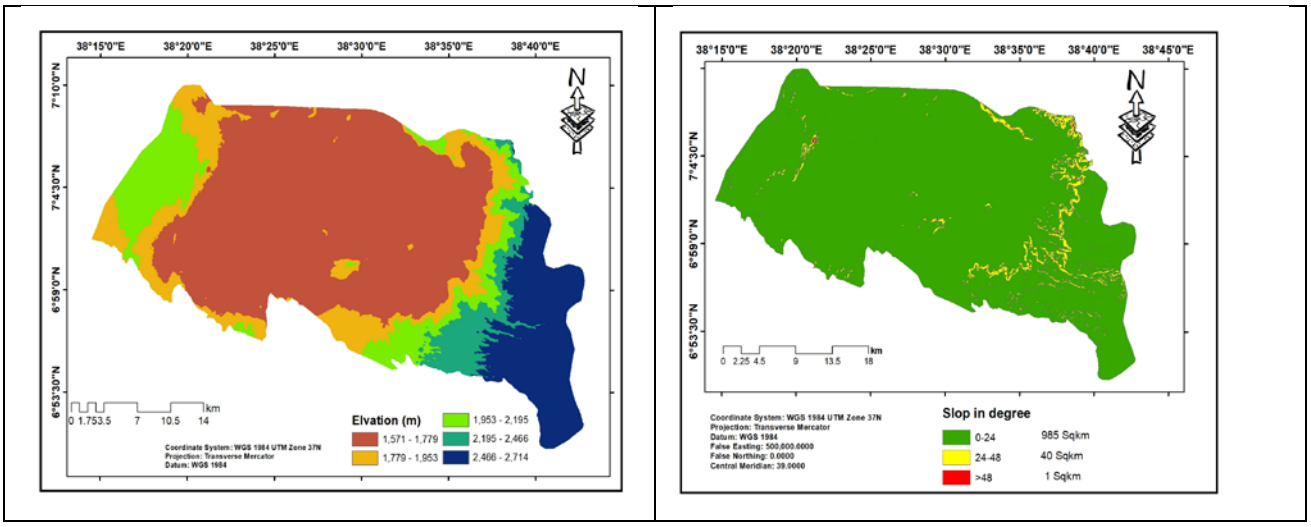

a) b)

Figure 3.2.(a) The study area's elevation and (b) slop maps of the study area

3.1.3. Climate and Vegetation

A. Temperature

The wet season in the Hawassa Area has a mean annual temperature of 19 °C. The dry season is characterized by year-round warmth and partly cloudy and overcast conditions. The annual average temperature rarely falls or rises above 9.4 °C or 33.3 °C and typically ranges between 12.2 °C and 30.5 °C. Figure.3 displays the long-term average monthly temperature distribution at the Hawassa meteorological station

B. Rainfall

Based on the rainfall record from the Hawassa meteorological station, the average annual rainfall is estimated to be 961 mm. Out of this total, 50% occurs during the Kiremt season (June-September), 20% during the Baga season (October-February), and 30% during the Belg season (March-May). The Ethiopian Meteorological Agency (NMA) has reported that the drier western regions receive 900 mm of rain per year, while the more humid eastern regions receive 1200 mm. Figure.3.3 illustrates the distribution of annual rainfall and temperature from 1988 to 2023.

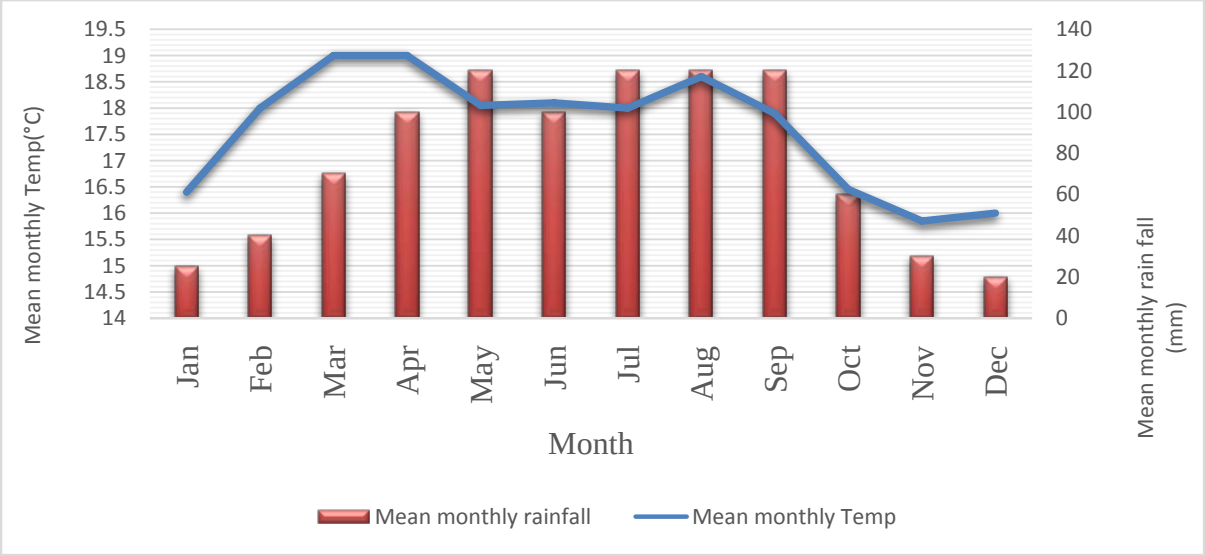

Figure 3.3.Distribution of mean monthly rainfall and temperature

C. Vegetation

The area's climate has a major influence on the spread of vegetation in the region tropical climate best describes the study area's conditions. There are two types of natural vegetation in the Hawassa region.In the eastern and north-eastern highlands of the region, mostly in Wendo Genet wereda and some in Malga wereda, thereis a damaged natural high forest. The second kind of vegetation is found in lowland acacia woodlands and bushlands, primarily in Hawassa Zuria weredas in the western portion of the region(Margareth, 2017).

3.1.4. Population

A total of 648,788 people live in the Hawassa area, according to CSA (2007). There are 317,551 female people and 331,237 male people in this population. Additionally, the total population is anticipated to be 792,027 based on 2017 central statistics authority (CSA) population projection statistics. Based on this, there are approximately 429,367 men and 411,713 women in the population. The specific details are shown in Fig. 3.4.

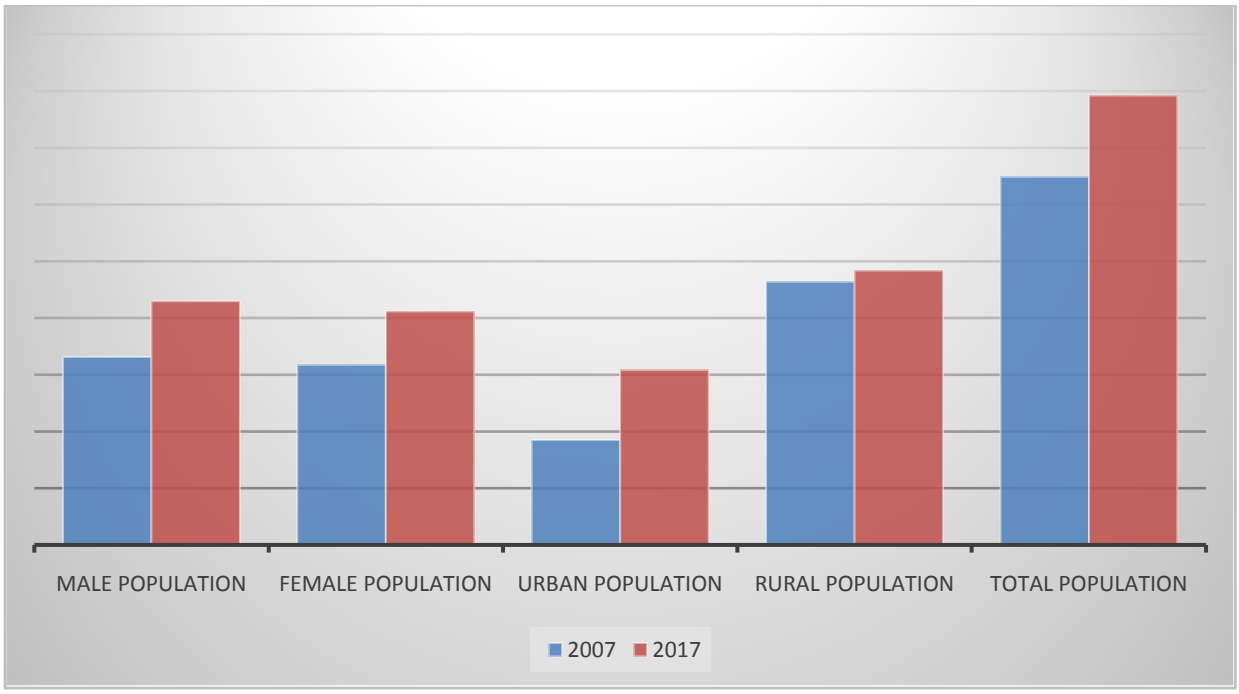

Figure 3.4. Population theHawassa area

3.2. Data and software

Primary and secondary (ancillary) data were both used in this study. The primary source is thebasic data, which is satellite data. Publications and governmental and nongovernmental organizations served as ancillary sources of data collection.

3.2.1. Primary data

The primary source of data is the satellite image, which was obtained from the European Space Agency (ESA) and the United States Geological Survey (USGS) in the following years: Thematic Mapper (TM) 1988, Enhanced Thematic Mapper Plus (ETM+) 2008, Thermal Infrared Sensor (TIRS) 2023, and Sentinel-2A Multi Spectral Instrument (MSI) 2023. To map the height and slope of the area, Digital Elevation Model (DEM) data with a resolution of 30*30 were merged with field data, GPS points, and images of various LU/LC classes.

3.2.2. Remote Sensing data acquisition

A single cloud-free image of the research area was obtained from the Earth Explorer website using satellite images from Sentinel-2A MSI (2023), Landsat 5 TM (1988), Landsat 7 ETM+ (2008), and Landsat 8 TIRS (2023). The Landsat images with path 168 and row 055 were used. The data was obtained from the Copernicus Data Space Ecosystem for Sentinel-2 from ESA and

usgs.gov, the United States Geological Survey (USGS). The projection system data used was the World datum (WGS84). Table.3. 1 shows the remote sensing images that were used to calculate the LST, NDVI, and LULC in the Hawassa area.

Table 3.1. Landsat and Sentinel-2A data used in the study area

Date of acquisition	Sensor	Path	Row	Multispectral Band	Thermal Band	Spectral range (micrometers)	Spatial Resolution (Pixel Spacing)	Source
Mar 15, 1988	TM	168	055	1-5& 7	6	0.45-12.50	30m and 120m	USGS
Feb 11, 2008	ETM+	168	055	1-6& 8	7	0.45- 12.50	30m, 60m and 15m	USGS
Feb 12 2023	TIRS	168	055	-	10&11	10.6-12.51	100m	USGS
Feb 17, 2023	MSI	168	055	2-4&8, 5-7&13-12, 1,10&11	-	0.43-2.20	10 m,20 m & 60 m	ESA

A. Landsat 5 Thematic Mapper (TM)

A satellite sensor that was a component of the NASA and USGS-run Landsat program was called Landsat 5 TM. Launched on March 1, 1984, and running until June 5, 2013, the Landsat 5 TM sensor transmitted nearly 2.5 million images of the world's land surface conditions while offering useful data for more than 28 years. The Landsat 5 TM sensor recorded seven spectral bands, encompassing the visible, near infrared, and thermal infrared regions of the electromagnetic spectrum.Landsat 5 had a temporal resolution of approximately 16 days, meaning it revisited the same location on average every 16 days.Table 3.3 presents comprehensive data.

Table 3.2.TM sensor bands and their description

Satellitesensor	Bands	Name	Wave Length inμm	Spatial resolution in meters	Temporal resolution	Source
Landsat 5 Thematic Mapper (TM)	Band 1	Blue	0.45-0.52	30	16 days	USGS
	Band 2	Green	0.52-0.60	30		
	Band 3	Red	0.63-0.69	30		
	Band 4	Near Infrared (NIR)	0.76-0.90	30		
	Band 5	Mid Infrared (MID) 1	1.55-1.75	30		
	Band 6	Thermal	10.40-12.5	120		
	Band 7	MIR 2	2.08-2.35	30		

B. Landsat 7 Enhanced Thematic Mapper plus (ETM+)

NASA and the USGS collaborated on the Landsat program, which featured the Landsat 7 ETM+ satellite sensor. The ETM+ is a stationary, multispectral scanning radiometer equipped with eight bands. It operates similarly to a "whisk-broom" and is capable of capturing high-resolution surface imaging data. It was in operation from April 15, 1999, until May 2013. When comparing Landsat 7 ETM+ to Landsat 5 TM, several enhancements were implemented.

The Landsat 7 ETM+ sensor was used to capture data in the visible, near-infrared, and thermal infrared parts of the electromagnetic spectrum. To address scan line gaps caused by an SLC malfunction, a Scan Line Corrector (SLC) was installed. Unfortunately, the SLC became ineffective in 2003 when there was a hardware malfunction, resulting in diagonal gaps in the images collected. It returns to the same spot on average every 16 days. Table 3.4 presents comprehensive data.

Table 3.3. ETM+ sensor bands and their description

Satellite sensor	Bands	Names	Wave length in μm	Spatial resolution	Temporal resolution	Source

				in meters		
Landsat 7 Enhanced Thematic Mapper Plus (ETM+)	Band 1	Blue band	0.45- 0.52	30	16 days	USGS
	Band 2	Green band	0.52- 0.60	30		
	Band 3	Red band	0.63- 0.69	30		
	Band 4	NIR band	0.77- 0.90	30		
	Band 5	MIR band	1.55- 1.75	30		
	Band 6	Thermal band	10.40-12.50	60		
	Band 7	MIR band	2.08 - 2.35	30		
	Band 8	Panchromatic	0.52-0.90	15		

C. Landsat 8 Operational Land Imager (OLI) and Thermal Infrared Sensor (TIRS)

Landsat 8 was launched on February 11, 2013. It is equipped with two sensors. The Operational Land Imager (OLI) sensor is manufactured by Ball Aerospace & Technologies Corporation, while the Thermal Infrared Sensor (TIRS) is made by the NASA Goddard Space Flight Center. The OLI sensor has a total of nine spectral bands, including a panchromatic band, with wavelengths ranging from 0.43 µm to 1.38 µm. On the other hand, the TIRS sensor consists of two spectral bands: one with a wavelength range of 10.6-11.19 µm, and another with a range of 11.5-12.51 µm. Detailed information is shown in Table 3.5.

Table 3.4.OLI/TIR sensor bands and their description

Satellite sensor	Band	Names	Wave length inµm	Spatial resolution in meters	Temporal resolution	Source
Lansat8 OLI and TIRS	Band 1	Aerosol	0.43 - 0.45	30	16 days	USGS
	Band 2	Blue	0.450 - 0.51	30		
	Band 3	Green	0.53 - 0.59	30		
	Band 4	Red	0.64 - 0.67	30		
	Band 5	NIR	(0.85 - 0.88	30		
	Band 6	SWIR 1	1.57 - 1.65	30		
	Band 7	SWIR 2	2.11 - 2.29	30		

	Band 8	Pan	0.50 - 0.68	15		
	Band 9	Cirrus	1.36 - 1.38	30		
	Band 10	TIRS 1	10.6 - 11.19	100		
	Band 11	TIRS 2	11.5 - 12.51	100		

D. Sentinel-2A Multi Spectral Instrument (MSI)

Sentinel-2, launched on June 23, 2015, is a part of the Copernicus program by the European Commission. This satellite is specifically designed to provide abundant data and imagery. It uses a multispectral sensor to analyze the visible, near infrared (VNIR), and short-wave infrared (SWIR) zones. With a resolution of 10 to 60 m, Sentinel-2A examines 13 spectral channels to detect changes in vegetation and capture high-quality atmospheric images. The Copernicus Sentinel-2 mission consists of a pair of similar satellites orbiting together.

Each satellite is equipped with a state-of-the-art wide-swath high-resolution multispectral imager that captures images in 13 different spectral bands. This cutting-edge technology provides a unique perspective on our environment and vegetation. The high-resolution spectral data is particularly valuable for monitoring crop growth and health, thereby enhancing agricultural productivity. Moreover, the geographical, temporal, and spectral advantages of various earth observation satellite sensors can be leveraged to combine Sentinel-2 satellite data with data from other earth observation satellites. By utilizing the strengths of multiple sensors in terms of geography, time, and spectrum, it is possible to merge the data from Sentinel-2 satellite with that from other earth observation satellites.Detailed information is shown in Table 3.6.

Table 3.5.MSI sensor bands and their description

Satellite sensor	Bands	Names	Wave length in µm	Spatial resolution in meters	Temporal resolution	Source
Sentinel-	Band S1	Coastal Aerosol	0.43 - 0.45	60	5 days	European
	Band S2	Blue	0.45 - 0.51	10		
	Band S3	Green	0.53-0.59	10		
	Band S4	Red	0.64-0.67	10		

2AMulti-Spectral Instrument (MSI)	Band S5	Vegetation Red Edge 1	0.69-0.71	20	Sentinel-2A, in combination with its twin satellite Sentinel-2B	Space Agency's (ESA) Copernicus program
	Band S6	VRE 2	0.73-0.75	20		
	Band S7	VRE 3	0.77-0.79	20		
	Band S8	NIR	0.78-0.90	10		
	Band S8A	Narrow NIR	0.85-0.88	20		
	Band S9	Water Vapor	0.94 - 0.97	60		
	Band S10	Cirrus	1.36 - 1.38	60		
	Band S11	Shortwave Infrared 1	1.57-1.66	20		
	Band S12	SWIR 2	2.10 - 2.29	20		

3.2.3. Ground truth data

For this work, GPS data was used as field data to accurately confirm the LU/LC classification of the image into several classes. It is important for both LU/LC categorization for multiple purposes evaluation of accuracy, gathering training data, class labeling, validation and calibration, and comprehension and interpretation. For all that purpose we collected nine(9) ground control points.

Several LU/LC class types are validated during field observation in the study area. Cropland (both large- and small-scale agricultural), forests, woody vegetation, grasslands, developed rural and urban settlements, wetland areas, and water bodies are among the classes under observation the map legends were created using the previously specified LU/LC classes, and GPS enabled training set data was necessary for image classification. Coordinates from sampling LU/LC classes and images of interesting scenes were taken during this ground truthing exercise.

3.2.4. Secondary data

Meteorological data, including average monthly rainfall and average monthly temperatures from 1988 to 2022, are examples of secondary data used in this study. These weather data were put to the test and confirmed.The Community Services Administration's demographic data was utilized to ascertain the population's status in the study area (CSA, 2007).

3.2.5. Data description and source

As indicated in Table3.7 below, primary and auxiliary data for this study were gathered from a variety of origin.

Table 3.6.Data presentation and source used in the study area

GIS data layer	Data presentation	Data source
Vector (polygon)	Wereda& Lake boundaries	Ethio-GIS
Vector (poly line)	Roads & Rivers	ERA_road2016 & Ethio-GIS
Vector (poly point)	Major city & town	Ethio-GIS
Attribute table	Rainfall & Temperature	National Metrological Agency (NMA)
Attribute table	Population	CSA 2007 &2017
Raster	Elevation & Slop	DEM 30m SRTM
Ground truth data	Ground truth 2023	Field survey
Raster	Satellite images ❖ Landsat 5 TM ❖ Landsat 7 ETM+ ❖ Landsat 8 OLI/TIRS ❖ Sentinel-2AMSI	USGS 1988,2008 ESA2023

3.2.6. Software Packages used

The software packages used for this work were ArcGIS 10.8 for image analysis, LST, NDVI, and map creation, and ERDAS Imagine 2015 for RS application to process satellite images, including image enhancement.ArcGIS pro 2.8 for supervised image classification, Google Earth was also used to verify and contrast findings with actual data, particularly for the LU/LC verification in the years 1988 and 2008.Quantum GIS (QGIS): raster manipulation was performed using open source software, which also included fixing Landsat 7 scan-line errors. Apart from the ERDAS Imagine software, word processing, spreadsheet analysis, graph creation, database management, and presentation were accomplished using Microsoft Office 2019, Excel, and PowerPoint. Mendeley workstation surface. Ink is utilized for reference and citation.

3.3. Methods

The present investigation commenced by procuring Landsat images for the years 1988, 2008, and 2023 from the Earth Explorer website (USGS). Additionally, Sentine-2A imagery for the

year 2023 was downloaded from ESA. The data was readily available, which is why these years were selected. The images that were downloaded or obtained were cloud-free and taken during the dry season. The study's overall methodological flow chart is displayed in Figure.8. Sentinel imagesare mostly being used in 2023 because of their fine spatial and temporal resolution, which is why we wish to use them. With a spatial resolution of 10 meters for its visible and near-infrared bands (bands 2, 3, 4, and 8) and 20 meters for its red-edge bands (bands 5, 6, and 7), Sentinel-2 satellites, including Sentinel-2A and Sentinel-2B, offer a greater spatial resolution than Landsat.

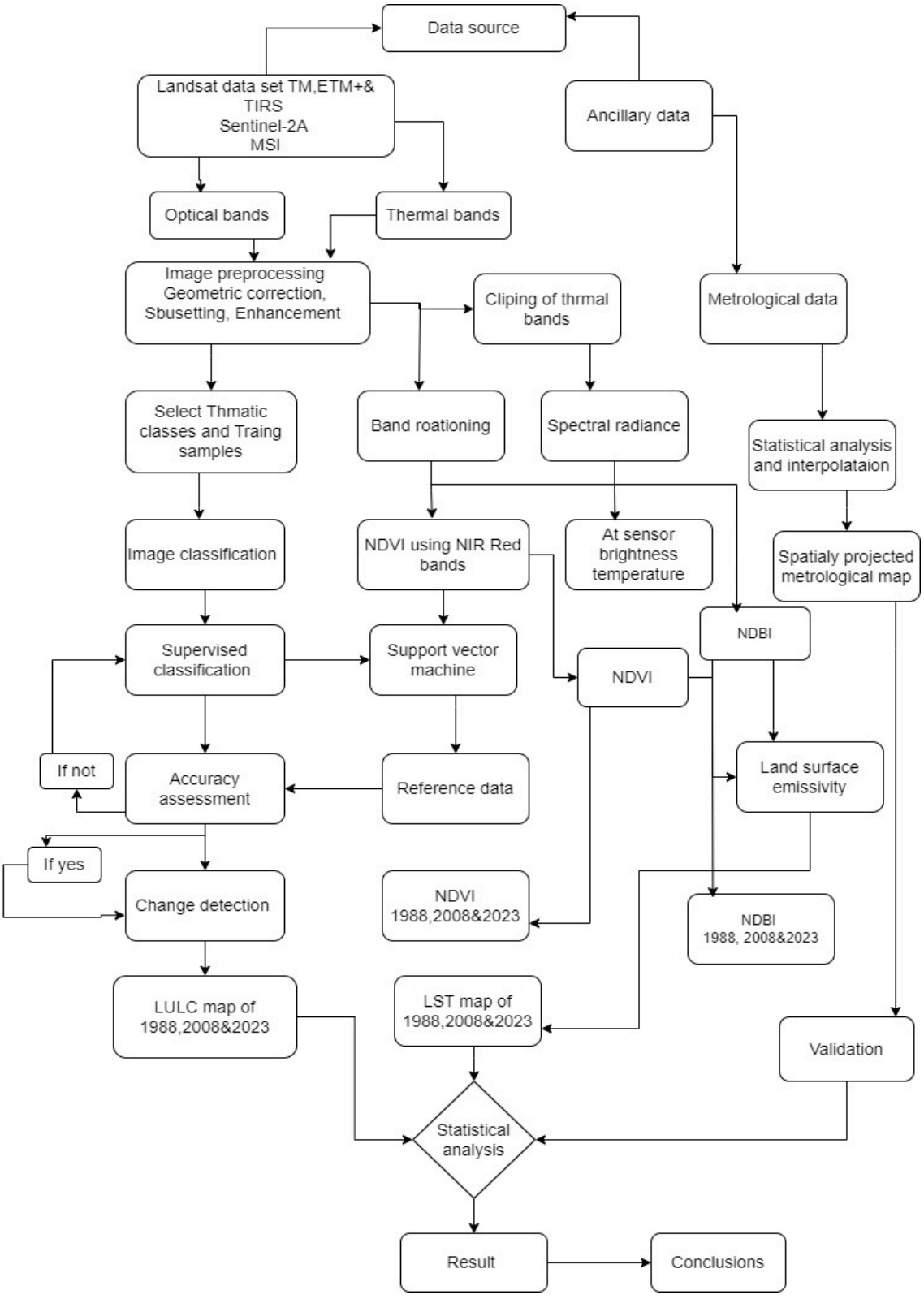

Figure 3.5. Analytical frame work

3.3.1. Data Preparation and Analysis

Preprocessing is the stage before further analysis to enhance the quality of the image. By their very nature, satellite images contain some haze, noise, distortion, and stripes. As a result, image preprocessing was carried out prior to data processing. Most typical data preparation procedures.

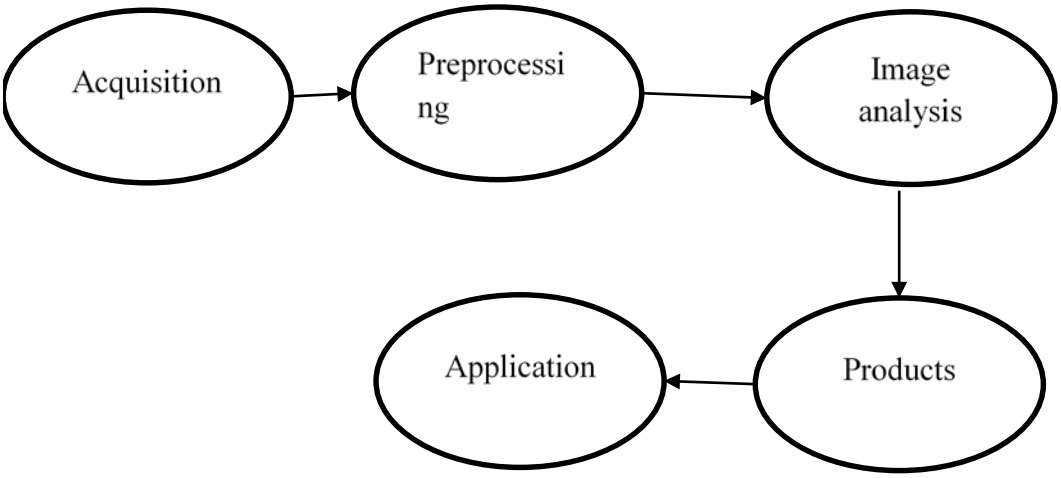

Figure.3.6. Remote sensing processing chain

The preprocessing stage encompasses various picture enhancing techniques such as pan sharpening, geometric correction, and radiometric correction, removing stripes, layer stacking, and sub-setting of the image based on the Hawassa region border.In order to make the ground truth conditions based on the sensors more representative, radiometric correction involves removing air noise.

Furthermore, the image was georeferenced by utilizing the Woreda border. The study used the WGS_1984_UTM_Zone_37N coordinate system for both raster and vector data during geo-referencing and re-projection processing.

3.3.2. Digital Image Processing (DIP)

Thanks to advancements in image processing, capturing, storing, and retrieving images from different sources has become much easier. The commonly used techniques in image processing include image restoration, image segmentation, image enhancement, de-noising, and de-blurring. Various imaging techniques such as computed tomography (CT), arterial spin labeling (ASL), magnetic resonance imaging (MRI), angiography, deep brain stimulation (DBS), and electroencephalography (EEG) greatly benefit from utilizing these images in different ways.

In the Image Processing applications mentioned above, mathematics has played a crucial role. Despite numerous breakthroughs and innovations, one area of imaging technology that has remained vital is the application of mathematics. It is evident that image processing and related topics share strong mathematical connections (Kalra et al. , 2022).

3.3.3. Image enhancement

The procedure of picture enhancement allows us to raise the digital image's quality, which facilitates feature identification. An image can be made brighter, sharper, or less noisy to achieve this (Bhardwaj et al., 2018).Image enhancement is one of the crucial image processing methods that can change one image into another to improve how much information is perceived by viewers that are human. During the process of acquiring and transmitting photos, external elements like illumination, equipment, and so on often affect the quality of the photographs. The purpose of image enhancement techniques was to enhance an image's quality or feature to the point where, when measured against a predetermined standard, the resultant image outperformed the original. The purpose of image enhancement methods was to enhance a feature or quality of an image so that when measured against a particular criterion, the final image is superior to the original (Rashed et al., 2021).

No single enhancement algorithm has shown to be successful with every kind of image. Enhancement algorithms' main goals were to lessen noise and increase the contrast between structures of interest and their surroundings. Furthermore, augmentation enhances and perfects image segmentation for both automatic systems and human interpretation, particularly in images where it is difficult to distinguish between normal and aberrant tissue (Bankman, 2009).

3.3.4. Image classification

The classification of satellite images is an essential component in the domains of Earth observation and remote sensing. It can be used for a wide range of tasks, including mapping land cover, monitoring the environment, managing disasters, urbanplanning, and evaluatingagriculture(Emad H.E. Yasin& Czimber Korne , 2023).

Based on the idea that various feature types on Earth's surface have unique spectral reflectance and remittance characteristics, the classification technique is utilized to identify these feature kinds. Image classification is the process of categorizing each pixel in an image or in

unprocessed remotely sensed satellite data in order to generate a certain set of labels or land cover themes (Al-Doski et al., 2013).Categorization is the final phase in the multi-step process of classifying satellite images, which starts with feature extraction.Creatingastrategy for the intended image classification is the first step in the sequential process of classifying images.

Subsequently, the images undergo preprocessing techniques like as image enhancement, scaling, grouping, and more. The third stage involves selecting the desired areas from those photos and creating the first clusters. Following that, the algorithm is used to classify the photos in the desired way, and the algorithm phasealso known as postprocessingis followed by the implementation of corrective measures(Mehmood et al., 2022).The last step is to evaluate how accurate this classification is, as Figure.9 illustrates. Supervised classification techniques are employed in this study.

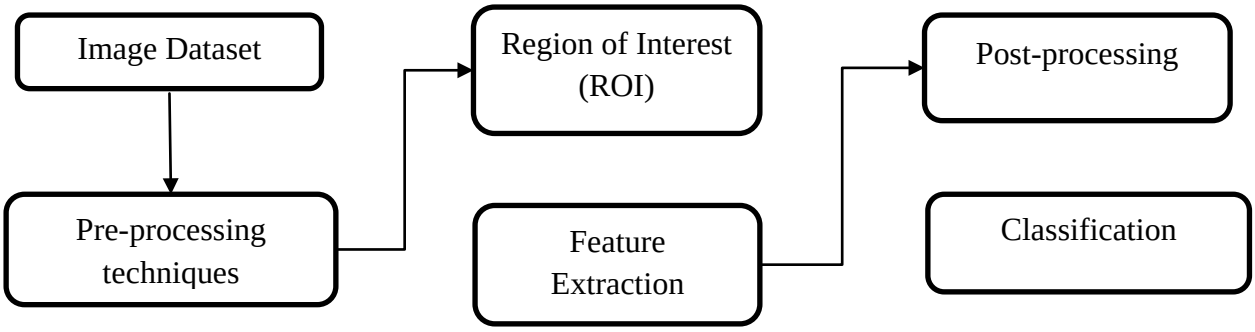

Figure 3.7. Remote sensing image classification process

A. Supervised image classification

The process of placing spectral classes into information classes is called classification. Groups of pixels in the various spectral channels of the data that are consistent in their brightness levels are known as spectral classes. Information classes are interest categories that an analyst looks for in the a picture based on his familiarity with the subject (Anand, 2018a).

In supervised classification, the analyst controls the image processing program and passes information to identify the relevant land cover classifications. Supervised image classification requires an analyst's input, which is known as the training set. The training samples that are used are one of the main elements of this technique. Accurate classification depends only on the training set.Two types of training samples are available: one is used for classification, and the

other is used to assess how accurate the classification is.To establish a classification determination rule, one must be aware of the spectrum properties or features pertaining to each class's population(Sathya & Baby-Deepa, 2017).

Following the completion of the training area designated for each class classification task,thirty (30) training sites were selected for the LU/LC kinds of agroforestry, cropland, woody vegetation, grasslands, and settlements (developed), while twenty (20) training locations were selected as samples for the LU/LC types of wetlands, forests, and water bodies.

Supervised classification using the ArcGIS Pro2.8 software's Support Vector Machine (SVM) classification method was used to map the LU/LC pattern using Multispectral Band, which included bands 1 to5 through 7 for TM 1988 and ETM+ 2008 and MSI 1 to5 and 8 through 13 bands of the preprocessed images. Image processing techniques are applied for the userspecified kind of land-use and land-cover classes in supervised classification. Agroforestry Crops, wetland, settlement, forest, grassland, woody vegetation, and water Body were the eight main classes examined in the Hawassa area. The creation of information classes, self-assessment through training sites, and reusable training sites were benefits of the supervised classification. On the other hand, information classes might not correspond with spectral classes, and information class uniformity and signature homogeneity might differ.

B. Support Vector Machine (SVM)

The machine learning technique known as SVM establishes the boundaries between data points using predetermined classes, labels or outputs. By carrying out ideal data transformations, it achieves this. SVMs are used to tackle challenging issues in outlier detection, regression, and classification.SVMs are widely employed in various fields, such as signal processing, natural language processing, speech and image recognition, and healthcare.

To best divide the data into the various classes, use a support vector machine classification, which maps the input data vectors into a higher-dimensional feature space.Large images can be processed by support vector machines, which also offer classification that is less susceptible to noise, correlated bands, or unequal distributions of training data.SVM, an effective supervised classification technique that can handle both a standard image and a segmented raster input, is

offered by the SVM classifier. Researchers utilize this classification technique rather frequently(Awad & Khanna, 2015).

Technically speaking, finding a hyperplane that cleanly divides the data points into distinct classes is the basic objective of the SVM method. The hyperplane positions itself to provide the largest margin of separation between the classes under consideration.

3.3.5. Classification accuracy assessment

The accuracy assessment of land cover for the years 1988, 2008, and 2023 was validated using 275 total samples points generating by using sampling strategy stratified random sampling. And a confusion matrix was calculated using ArcGIS 10.8 software.

When evaluating a map qualitatively, you compare what you see on the ground with what you see on the map or image to see if it seems correct. On the other hand, quantitative evaluations aim to detect and quantify map inaccuracies derived from remote sensing data. In these evaluations, ground truth datawhich is believed to be 100% accurate is compared to map data(Anand, 2018b).The accuracy of the LU/LC classification was evaluated through the use of Google Earth and a field study by.The final classification accuracy output was computed for the LU/LC maps years 1988, 2008, and 2023. Table 8 lists the kinds of land use and land cover along with a description of each.

Table 3.7. LU/LC classes and their description

LU/LC Classes	Description
Cropland	Land utilized for growing crops. The total area classified as "Permanent crops" and "arable land" (FAO definition of categories).
Settlement	A human settlement is any collection of houses, regardless in size or form, inhabited by people.
Forest	More than 0.5 hectares of land with trees that are at least 5 meters tall and have a canopy cover of 10% or greater, or trees that can to reach these criteria naturally.
Grass land	A grassland is a region where an almost constant grass cover dominates the vegetation.
Water body	A lake, stream, river, or a portion of a stream or river is an example of a clearly identifiable surface water body.
Woody Vegetation	Woody vegetation is defined as sections that are 300 feet or fewer from a surface stream and comprise one acre or more of shrub or open or dispersed forest canopy (less than 60% crown closure).

Wet land	Wetlands are places where water either covers the soil or is present at or near the soil's surface year-round or for different parts of the year, including the growing season.
Agroforestry	An intermediate land use technique known as agroforestry (AF) blends the ecosystem qualities of pastures, farmland, and forests by planting trees or shrubs alongside them.

3.3.6. Changes detection in LU/LC

Observing something or a situation reputedly in order to identify any change in its state (Singh, 1989).LU/LC change detection was carried out using 1988, 2008, and 2023 images. Thematic images comparisons were made using GIS tools. A cross-operational process called "mapping LU/LCC across time" began with mapping the most recent satellite images from 2023 and then went back in time to map the imagery from 1988.Post categorization is one of the most popular techniques for change detection(Chen, 2002).ArcGIS software approaches were utilized for technical procedures of integration in the study of LU/LCC maps. Creating a table with the area covered in square kilometers and the percentage change for each of the three years 1988, 2008, and 2023 in relation to each other was the first assignmentthe percentage equation (eq.3.1) was utilized to compute LU/LCC(Lambin et al., 2001).

$$\text{Percentage} = \frac{\text{Observed change}}{\text{Sum of area}} * 100 \quad \text{Eq. (3.1)}$$

3.4. Derivation of Normalized Difference Vegetation Index

The NDVI is arguably the most popular remote sensing spectral index for monitoring Earth's surface. The index utilizes the leafs of optical properties, which chlorophyll and other pigments absorb visible light for photosynthesis and reflect NIR light(Robinson et al., 2017). The range of the NDVI value was -1.0 to +1.0. High near-infrared reflectance and low red-light reflectance in healthy plants result in high NDVI values. The increasing number of positive NDVI readings shows that there is more green vegetation present.The NDVI is developed with red and near infrared bands because red is greatly influenced by chlorophyll content and near infrared is linked to leaf cell structure and air gaps inside the leaf.The cell structure of leaves changes with growth and maturity, and this can have a significant impact on near-infrared scattering (Patón,

2020).Therefore, we may determine what is occurring with the plant by using Equation 3.2,this measures the proportion of red to nearinfrared light.

$$NDVI = \frac{NIR - Red}{NIR + Red} \quad \text{Eq. (3.2)}$$

Where

NDVI = normalized difference vegetation index

NIR = while Landsat 8's near-infrared band is represented by band 5 and red band as well as band 4, Landsat 5&7's near-infrared band is represented by band 4 and red band as well as band 3.

Fractional vegetation cover, or FVC, is the ratio of the overall vegetation area to the vertical projection area of vegetation (leaves, stalks, and branches) on the ground. FVC is an important biophysical parameter when utilizing the soil vegetation-atmosphere transfer model to simulate the exchange between the land surface and the atmospheric boundary level(Salimi Kouchi et al., 2013).For FVC, the following Eq. 3.3 was used:

$$FVC = \frac{NDVI - NDVIs}{NDVIv - NDVIs} \quad \text{Eq. (3.3)}$$

Where

FVC = fraction of vegetation cover

NDVI= normalized difference vegetation Index

NDVIv = NDVI for vegetation and NDVIs = NDVI for soil

Equation 3.4 was used to calculate Proportion of Vegetation that helps in calculating Landsat 8 land surface emissivity (LSE).

$$PV = \frac{(NDVI - NDVImin}{(NDVImax - NDVImin)} \quad \text{Eq. (3.4)}$$

Where

PV = proportion of vegetation

NDVI=normalized difference vegetation index

NDVI min= normalized Difference vegetation index minimum value

NDVImax= normalized difference vegetation index maximum value

3.5. Derivation of Normalized Difference Built -UP Index

Through altering land cover, urbanization, deforestation, desertification, natural disasters, and intensive agricultural practices have a substantial impact on regional and global climate characteristics.These alterations typically lead to rises in near-surface temperatures and the creation of heat islands, which in turn cause various meteorological phenomena (Osgouei et al., 2019).You can create the equation (eq 3.5) that follows to distinguish NDBI areas from other kinds of LC.The NDBI has values between -1 and +1. A positive figure denotes an urban or built-up area.This is due to the fact that urban areas often reflect more light in the SWIR band than in the NIR range. Negative value show water bodies because the NIR and SWIR bands have very low reflectance for with NIR band often reflecting slightly more than the SWIR.

$$NDBI = \frac{SWIR - NIR}{SWIR + NIR} \quad \text{Eq. (3.5)}$$

Where

NDBI = normalized difference built up index

SWIR = short wave infrared

NIR = near infrared

3.6. Derivation LST

Satellite remote sensing measures variations in LST in space and time, which are used to estimate a wide range of geophysical parameters, including evapotranspiration, vegetation water stress, soil moisture, and thermal inertia(Rozenstein et al., 2014).Table 9 lists the values of the emissivity constant for soil and vegetation.

Table 3.8. Emissivity constant value for Landsat 8

Emissivity type	Band10	Band11

εs	0.971	0.977
εv	0.987	0.989

The following three formulas are used to compute the land surface emissivity (LSE), mean of LST, and change of LSE of Bands 10 and 11, in that order:

$$LSE = 0.004pv + 0.98 \quad \text{Eq. (3.6)}$$

$$\text{Mean of LST} = \frac{LST\,10 + LST\,11}{2} \quad \text{Eq. (3.7)}$$

$$\text{Difference LSE} = LSE10 - LSE11 \quad \text{Eq. (3.8)}$$

3.6.1. Radiometric correction

A set of techniques known as "radiometric correction" is used by researchers and analysts to translate digital sensor data into physically meaningful quantities, such brightness, surface temperature, or reflectance(K. Liu et al., 2020). The spectral radiance can be obtainedbyapplyingthe following equation.

To convert digital numbers:

$$L\lambda = Lmin + (Lmax - Lmin) * \frac{DN}{255} \quad \text{Eq. (3.9)}$$

Where

L λ=Spectral radiance

Lmin=Spectral radiance of DN value 1

Lmax=Spectral radiance of DN value 255

DN = digital number

3.6.2. Conversion at sensor spectral radiance

Pixel values, denoted by Q in the unprocessed, raw remote sensing image data, were converted into absolute radiance values in radiometric calibration. The sensor spectral radiance or satellite data scaled into 8 bits was converted using equation 3.9.

$$L\lambda = \left(\frac{Lmax\,\lambda - Lmin\,\lambda}{Qcalmax - Qcalmin}\right)(Qcal - Qcalmin) + Lmin\lambda \quad \text{Eq. (3.10)}$$

Where

L λ= the computed radiance linked to the ground area within each pixel and associated with the λ wavelength range of a particular band, or the spectral radiance at the sensor's aperture.

Lmaxλ=spectral at the Qcalmax-scaled sensor radiance

Lminλ=spectral at the Qcalmin-sensor radiance

Qcalmax=the maximum quantized calibrated pixel value corresponding to Lmaxλ

Qcalmin=minimum quantized calibrated pixel values that much Lminλ

Qcal=quantized calibration pixel value

3.6.3. Conversion to top of atmosphere (TOA) reflectance

The reflectance that a space-based sensor that is orbiting above the earth's atmosphere measures is known as top-of-atmosphere reflectance, or TOA reflectance. Clouds, atmospheric gases and aerosols will contribute to these reflectance values.Data processing and adjustments are required for Landsat Thematic Mapper top of atmospheric reflectance because of the temporal lag between data collection and solar zenith angle variation. To compute TOA, Equation 3.10 was utilized.

$$P\lambda = \frac{\pi * L\lambda * d^2}{ESUN\,\lambda * \cos\,\theta S} \quad \text{Eq. (3.11)}$$

Where

Pλ= the planetary top of atmosphere (TOA) reflectance is either unit less or lacks a unit.

P= is a mathematical constant with a rough value of 3.14159. Additionally, it is unit less.

Lλ=spectral radiance at the sensor’s aperture

d^2=astronomical units for the distance between the sun and the earth

ESUNλ=mean solar radiation at the Exo-atmospheric layer (from Meta data)

3.6.4. Conversion of radiance into brightness temperature

The temperature of brightness T_b, or radiant temperature, has been widely utilized for thermal infrared measurements based on remote sensing and ground observations. The temperature of a blackbody is equal to the surface temperature (T_b) when the radiation emitted from the surface equals that of a blackbody. Thermal constants included in the Meta data file can be used to translate thermal infrared data from effective sensor brightness temperature (TB) to atmospheric reflectance (Lλ). Band 6 on thematic mapper and enhanced thematic mapper plus, which corresponds to the thermal band of Landsat images, needs to be adjusted from effective at sensor brightness temperature to sensor spectral radiance. Equation 3.11 was utilized to convert Lλ (spectral radiance) to TB (brightness temperature),(Rajeshwari,A., and Mani,N., 2014).

$$TB = \left(Ln\frac{\frac{K2}{K1}}{L\lambda}\right) + 1 \quad \text{Eq. (3.12)}$$

Where

TB=efficient at the Kelvin unit of satellite brightness temperature

K2=calibration constant 2

Ln=natural logarithm

K1=calibration constant 1

L=spectral radiance at thesensor's aperture

Thermal bands 10 and 11, which are collected at 100 meters but resampled to 30 meters during Level-1 product creation, are helpful in delivering more precise surface temperatures. Images from the TIRSand Landsat 8 OLI have nine spectral bands.The calibration constant used to calculate the brightness temperature is displayed in Table 10.

Table 3.9. Thermal band calibration constant of Landsat 8

Satellite	Sensor	Categories	Band 10	Band 11
Landsat8	TIRS	K1	774.89	480.89
		K2	1321.08	1201.14
		Radiance_ MULT_BAND	0.0003342	0.0003342

		Radiance_ADD_BAND	0.01	0.01

Using band 10 and 11 of the split window algorithmfirst proposed by Mc Millin in 1975,LST was produced from Landsat TIRS. In this manner (eq.3.12).

$$LST=TB10+C1\ (TB10-TB11)+C2\ (TB10-TB11)^2+C0+(C3+C4W)\ (1-m)+(C5+C6W)\ \blacktriangle m \quad \text{Eq. (3.13)}$$

Where

LST=land surface temperature

C0 up to C6=split window coefficient value

TB10=Band's brightness temperature Brightness Temperature of Band11 = 10 TB11

m=Mean Land Surface Emissivity of thermal infrared bands (mean of band 10 and 11)

W=The Earth Science Reference Table (ESRT) provides the atmospheric water vapor content (0.005) and the relative humidity table.

▲m = difference in land surface emissivity (LSE)

During performing/calculating the LST of a given area, Landsat 8 thermal bands (Table 11) were used.

Tabl.3.10.Split window algorithm constant value

Constant	Value
C0	-0.268
C1	1.378
C2	0.138
C3	54.3
C4	-2.238
C5	-129.2
C6	16.4

Landsat 8 calibration constant differs from that of Landsat 5 and 7. The Landsat 5 and Landsat 7 cases were handled using Table12.

Table 3.11.TM and ETM+ thermal band calibration constants

satellite	sensors	constant	value
Landsat 5	TM	K1	607.76
		K2	1260.5
Landsat 7	ETM+	K1	666.09
		K2	1282.71

The temperature was converted from degree Kelvin to degree Celsius by deducting 272.15 from the result. Therefore, the formula below (eq.3.13) was employed to convert degrees Kelvin to degrees Celsius.

$$C = K - 272.15 \quad \text{Eq. (3.14)}$$

Where

C: result in degree Celsius

K: result in degree Kelvin

3.7. Zonal statistics

The values of raster cells falling inside zones defined by another raster or vector dataset are used to compute zonal statistics. Zonal statistics summarize the value of a specific set of cells. For comparing one zone to another and occasionally between various cells within a zone, zonal statistics might be helpful. Additionally, they provide a practical means of tracking patterns and evaluating advancement over time in different zones or geographical areas

LU/LC, NDVI, and LST maps were created for the years 1988, 2008, and 2023. The spatial difference of LST based on different LU/LC classifications was examined using the ArcGIS 10.8 zonal statistics tools, and the results were presented. The summary statistics of the LU/LC, NDVI, and LST map data were then evaluated using Excel. The use of zonal data as a table is a significant technique for analyzing the relationship between LU/LC and LST. Zonal statistics

result in a new raster or table that provides summary statistics of the input raster for the specified zones.

3.8. Spatial Analysis (interpolation)

A technique called spatial interpolation uses measurements from nearby known pixels or from within a range of unknown pixels to approximate the value of unknown pixels. According to Tobler's First Law of Geography, locations that are close to each other in space are more likely to have similar values than those that are far apart. In this study, meteorological data was used for interpolation, analysis, and comparison with Landsat thermal infrared band LST values. The temperature was interpolated using the Inverse Distance Weighted (IDW) method.

IDW is a straightforward interpolation technique that doesn't call for variogram modeling. The distance from the sampled sites to the value of a variable at an un-sampled location is assumed to be inversely proportional by IDW.In other words, the interpolation assigns more significance to a sampled site when it is closer to the un-sampled location.IDW uses a power parameter to regulate the rate of reduction in weight with distance. A greater effect from the closest neighbors is indicated by a higher power parameter, whereas greater smoothing and averaging of the interpolation is caused by the farther neighbors.Thus, in the current investigation, sample points were utilized to interpolate temperature data in the ArcGIS 10.8 environment. The resulting interpolated maps were then used for validation.

CHAPTER FOUR

4. RESULTSand DISCUSSION

4.1. Land-use/land-cover in 1988, 2008 and 2023

In 1988, the results of land cover classification revealed that the main land cover categories were agroforestry, cropland, and woody vegetation. These three classes collectively covered 71% of the total area. Specifically, out of the entire area of 1026.5 km^2, agroforestry covered 158.7 km^2 (15%), cropland covered 439 km^2 (42.79%), and woody vegetation covered 133.7 km^2 (13%).The remaining land consists of forests, grasslands, settlements, water bodies, and wetlands, totaling 295km^2 (28%). Among all the LU/LC classes, forests have the smallest area coverage.

Table 4.1.Change in Land Use/Land Cover (1988-2023) and its rate of change in the Hawassa Area.

Land use and land cover area coverage and their net change from 1988 to 2023									
LU/LC class	1988		2008		2023		1988-2008	2008-2023	1988-2023
	Area (km^2)	Area (%)	Area (km^2)	Area (%)	Area (km^2)	Area (%)	Area (km^2)	Area (km^2)	Area (km^2)
Agroforestry	158.70	15.45	125.29	12.20	128.79	12.53	-33	3.5	-29.91
Cropland	439.45	42.79	419.97	40.9	312.58	30.42	-19	-107	-126.8
Forest	22.87	2.23	26.50	2.58	30.00	2.92	3.63	3.5	7
Grassland	59.14	5.76	80.00	7.79	88.73	8.64	20.89	8.7	29.6
Settlement	26.00	2.54	46.30	4.50	51.5	5.01	20.21	5	25.44
Water body	94.9	9.24	94.10	9.16	93.9	9.14	-0.8	-0.2	-0.97
Wetland	92.00	8.97	112.70	10.98	114.5	11.15	20.6	2	22.51
Woody vegetation	133.70	13.00	122.00	11.88	207	20.18	-11.72	85	73.67
Total	1026.5	100	1026.5	100	1026.5	100			

The 2008 results revealed that cropland covered the largest area in the study region, measuring 419.97 km^2 (40.90%). This was followed by agroforestry and woody vegetation, accounting for 125.29 km^2 (12.20%) and 122.00 km^2 (11.88%) respectively. The remaining land cover types, including forest, grassland, settlement, water bodies, and wetland, accounted for 359.60 km^2

(35%) of the total area. Similarly, in 1988, forests occupied a smaller area compared to all other categories. The categorization techniques using the 2023 Sentinel-2A MSI data were employed in developing the land cover maps.

The results of the land cover classification in 2023 showed that cropland, woody vegetation, and agroforestry covered a total area of 648.7 km^2 (63%). The remaining land cover types, including forest, grassland, settlement, water body, and wetland, accounted for 378.7 km^2 (36.8%). It was observed that cropland consistently decreased from 1988 to 2023.However, from 1988 to 2023, there was a consistent increase in grassland, settlement, and wetland areas. Detailed statistical information for each of these categories, as well as the LU/LC map for the entire study period, can be found in Table4.1 and Figure 4.1.

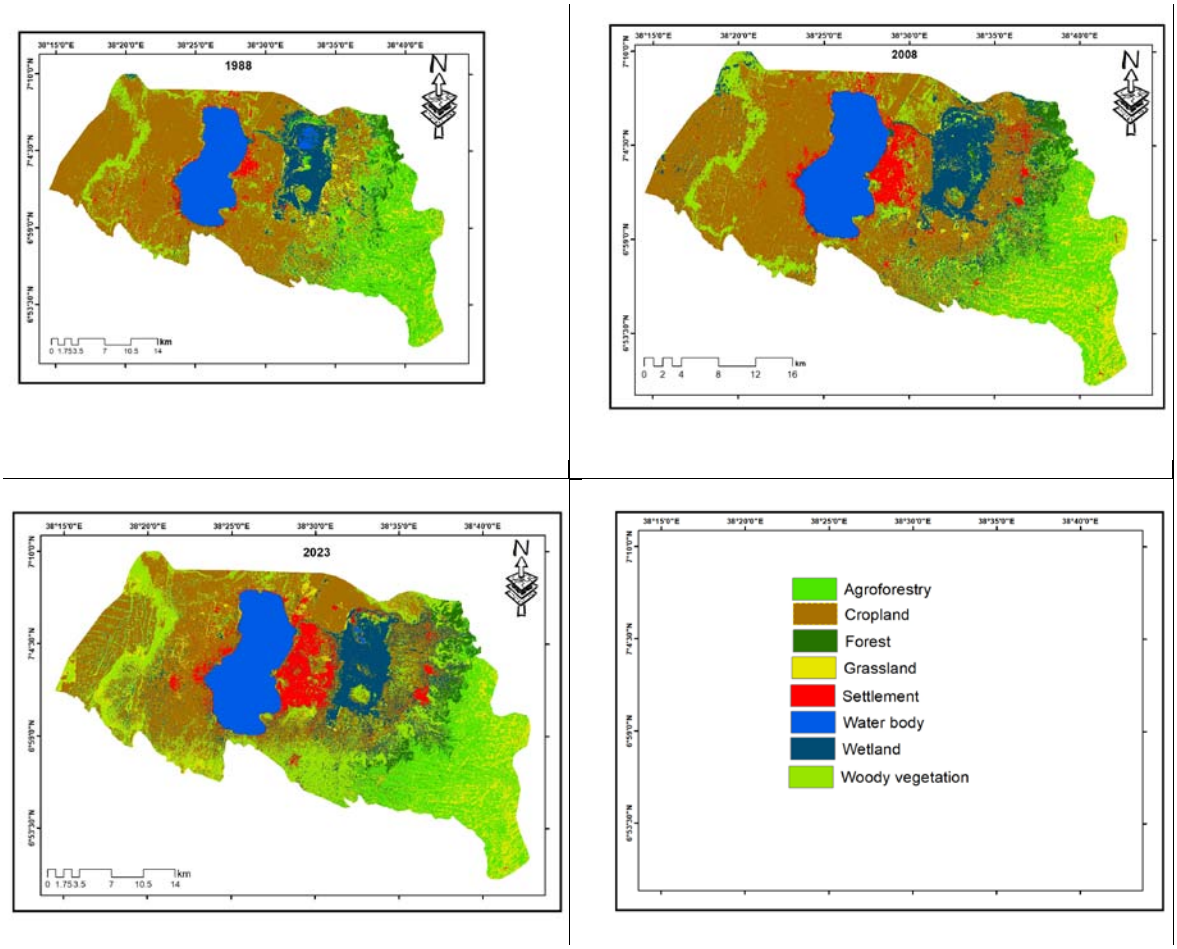

Figure.4.1.LU/LC map of the study area for the years 1988, 2008, and 2023.

From 1988 to 2023, the research area's maximum extension of LU/LC was found in the class of cropland. Cropland area fell from 439.45 km^2 in 1988 to 312.58 km^2

4.2. The study area's spatial distribution and coverage of LU/LC types.

The forest land has steadily and slowly increased over the years from 1988 to 2023. It started at 2.23% in 1988, then grew to 2.58% in 2008, and finally reached 2.92% in 2023. Similarly, the grassland area also experienced an increase, going from 5.76% in 1988 to 7.79% in 2008, and further rising to 8.64% in 2023.Another notable change in the research area is the steady growth of settlements, which started at 2.54% in 1988, then climbed to 4.5% in 2008, and finally reached 5% in 2023.From 8.97% in 1988 to 10.98% in 2008 and 11.2% in 2023, wetland also increased.Water body decreased from 9.24 in 1988 to 9.16 in 2008 and 9.14% in 2023, a moderate and steady decline. There were variations in agroforestry and woody vegetation between 1988 and 2023. In 1988, the percentage of agroforestry was 15%; by 2008, it had dropped to 12.20%; and by 2023, it had risen to 12.53%. The percentage of woody vegetation has also altered, rising from 13% in 1988 to 11.88% in 2008 and then to 20.18% in 2023. From 42% in 1988 to 40.90% in 2008 and finally to 30.42% in 2023, cropland fell

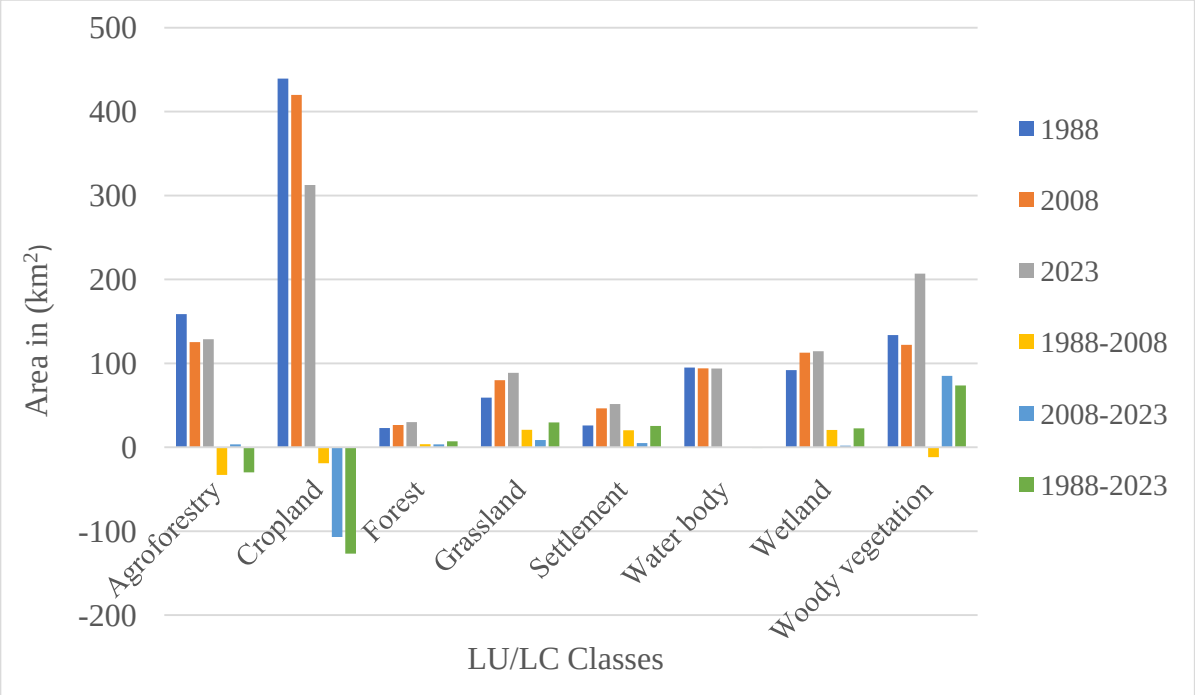

Figure.4.2.LU/LC distribution and net changes during (1988-2023)

Table.4.2.LU/LC change matrix of the Hawassa area (km^2)

					2008					
		Agroforestry	Cropland	Forest	Grassland	Settlement	Water body	Wetland	Woody vegetation	Total
1988	Agroforestry	**88.84**	7.13	8.19	8.99	2.76		3.45	8.59	125.21
	Cropland	9.86	**332.08**	0.35	9.25	7.97	0.011	13.28	47.03	419.85
	Forest	6.18	1.72	**10.41**	0.25	0.035	0.037	3.055	4.78	26.49
	Grassland	33.91	6.51	0.278	**27.98**	0.137		5.88	5.24	79.96
	Settlement	0.96	24.39	0.0131	0.55	**11.59**	0.026	1.22	7.47	46.24
	Water body	0.0022	0.206	0.022	0.042	0.80	**90.31**	1.82	0.89	94.10
	Wetland	10.32	19.51	1.51	10.12	0.96	4.02	**53.20**	13.10	112.69
	Woody vegetation	8.54	47.70	2.10	1.90	4.53	0.49	10.14	**46.56**	121.94
	Total	158.634116	439.279573	22.8435896	59.1130641	26.0383752	94.8971799	92.0523514	133.6528863	**1026.51114**

4.3. Expansion of settlements from 1988 to 2023

An overlay analysis of settlement areas found in the Hawassa area on satellite image taken in 1988, 2008, and 2023 showed that the area's grassland, agroforestry, cropland, and woody vegetation had all been converted to settlement areas in a different direction. The change in Hawassa City's administrative status was linked to the built-up area's fast expansion. Hawassa was progressively evolved to the municipality level in historical development on May 20, 1995 E.C. Figure.14 illustrates how the settlement area has expanded to include various LU/LC classes.

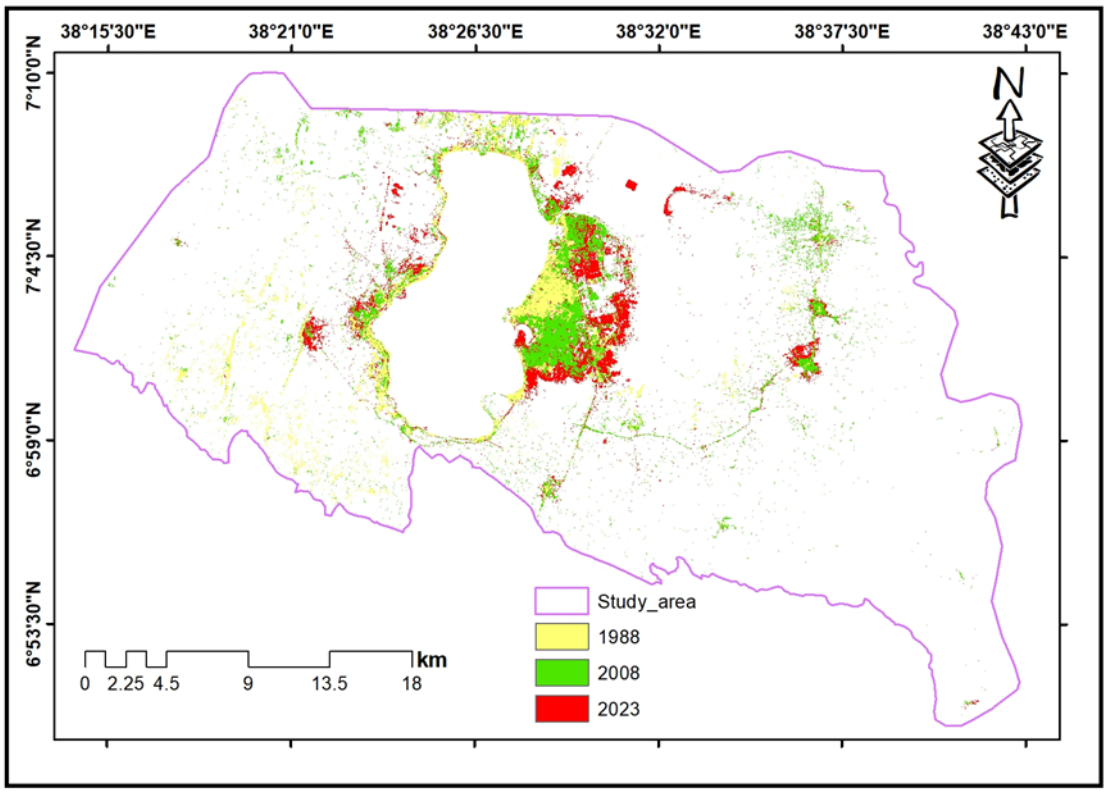

Figure.4.3. trend of settlement expansion from the year 1988-2023 in Hawassa area

4.4. Assessment of accuracy

This assessment was conducted using ArcGIS 10.8 and stratified random sampling strategy approaches for each research year. The overall categorization accuracy for LU/LC in 1988, 2008, and 2023 was found to be 88%, 86%, and 92% respectively. The categorization Kappa statistics for 1988, 2008, and 2023 were determined to be 0.8517, 0.8241, and 0.9036 respectively. For precise information on producers and users' accuracy, please refer to Table 16.

Table.4.3. Statistics on the accuracy assessment for 1988, 2008, and 2023

	1988		2008		2023	
Class name	Producer's accuracy (%)	User's accuracy(%)	Producer's accuracy(%)	Users accuracy (%)	Producer's accuracy(%)	Users accuracy (%)
Agroforestry	87.23	80.17	82.05	96.96	94.28	97.05
Cropland	98.93	70.00	82.05	83.78	93.90	92.77

Forest	98.93	100.00	82.05	80.00	100.00	100.00
Grassland	98.93	100.00	82.05	86.36	100.00	91.66
Settlement	98.93	84.00	82.05	76.92	60.00	85.71
Water body	98.93	96.00	82.05	92.00	100.00	100.00
Wetland	98.93	97.29	82.05	90.32	92.59	80.64
Woody vegetation	98.93	80.17	82.05	79.41	91.07	91.07
Overall Accuracy	88.25		86.02		92.00	
Kappa Coefficient	0.8517		0.824128		0.903617	

4.5. SpatialTemporal distribution of NDVI

According to the study, a maximum NDVI value of 0.51 in 1988 indicates a moderate density of vegetation. This suggests that while the vegetation in the study area was not at its densest, it was still in good health. The maximum NDVI value increased to 0.56 by 2008, indicating an improvement in both density and vitality compared to 1988. However, the maximum NDVI value decreased to 0.48 in 2023 from 0.56 in 2008. Although slightly lower than the peak in 2008, this rating still indicates healthy vegetation with some level of density. The slight decline observed may indicate slight differences in plant density or health. Results from the normalized difference vegetation index (NDVI) in 1988, 2008, and 2023 showed higher values in the eastern and southeastern parts of the research area. On the other hand, the western portion of the study area displayed comparatively lower NDVI values. Statistical information for the NDVI values in 1988, 2008, and 2023 is presented in Table 17.

Table.4.4. NDVI value statistics for the years 1988, 2008, and 2023

Year	Minimum	Maximum	Mean	Standard deviation
1988	-0.2089	0.5195	0.190	0.1115
2008	-0.3725	0.5657	0.080	0.1575
2023	-0.0699	0.4875	0.1745	0.1154

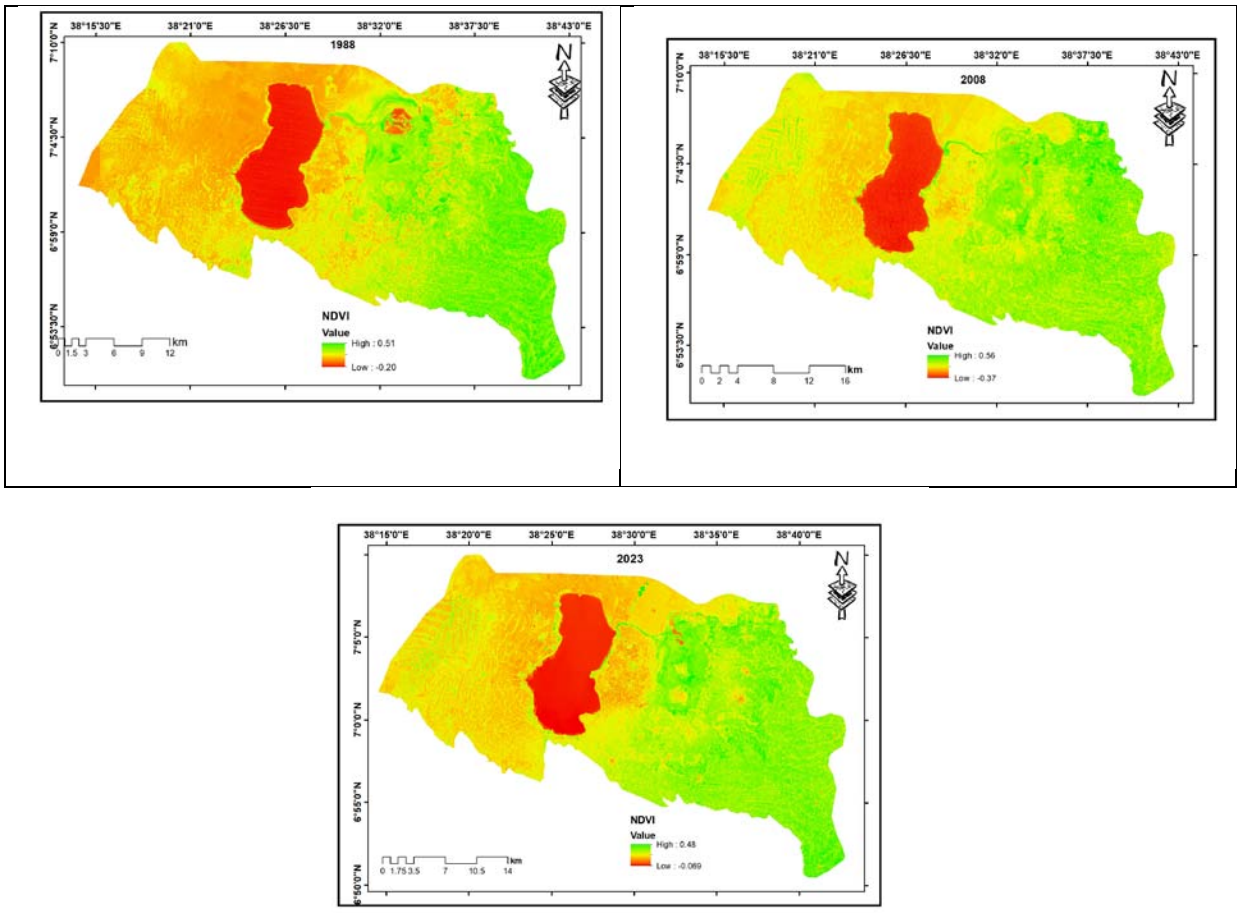

Figure.4.4. NDVI maps of the study area (1988, 2008, and 2023)

4.6. Normalized difference Built -up index

The greatest NDBI score of 0.24 in 1988, according to this study, indicates a comparatively low level of built-up areas. This lower figure suggests that urbanization was not as widespread at this time. There were probably more natural land cover categories in the terrain, like vegetation, water features, and undeveloped land. The maximum NDBI value increased to 0.41 by 2008, indicating a strong expansion of built-up or urban areas throughout the 20-year period from 1988 to 2008. Compared to previous years, the NDBI score of 0.63 in 2023 indicates a substantial increase in built-up areas. This suggests that between 2008 and the present year, there was a significant surge in urban development and expansion. Table 18 displays the statistical data for the NDBI values in 1988, 2008, and 2023.

Table.4.5. Statistical information on NDBI value for the years 1988, 2008, and 2023

Year	Minimum	Maximum	Mean	Standard deviation
1988	-0.33	0.24	0.00	0.10
2008	-0.47	0.41	0.05	0.12
2023	-0.37	0.63	0.03	0.10

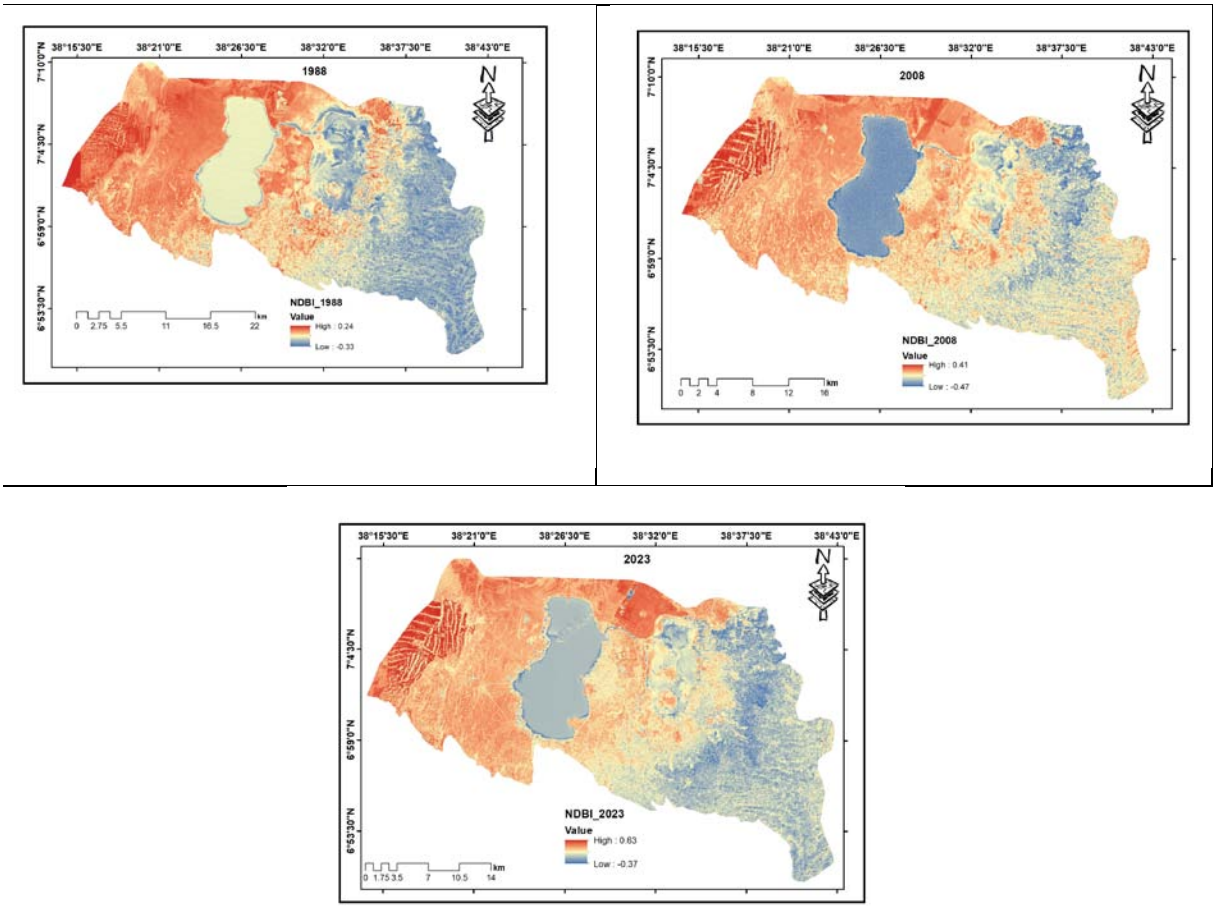

Figure.4.5. NDBI maps for the years 1988, 2008, and 2023 of the study

4.7. Relationship between LU/LC and NDVI

During the research periods, NDVI maps were generated using red and near-infrared bands, revealing varying NDVI values based on different types of land cover. The NDVI serves as an indicator of vegetation health, thus its readings differ from one location to another depending on the level of vegetation present. Forested areas, with their dense canopy, green leaves, and

abundant chlorophyll, showed high NDVI readings. Similarly, agroforestry and regions covered by forests exhibited higher NDVI values.

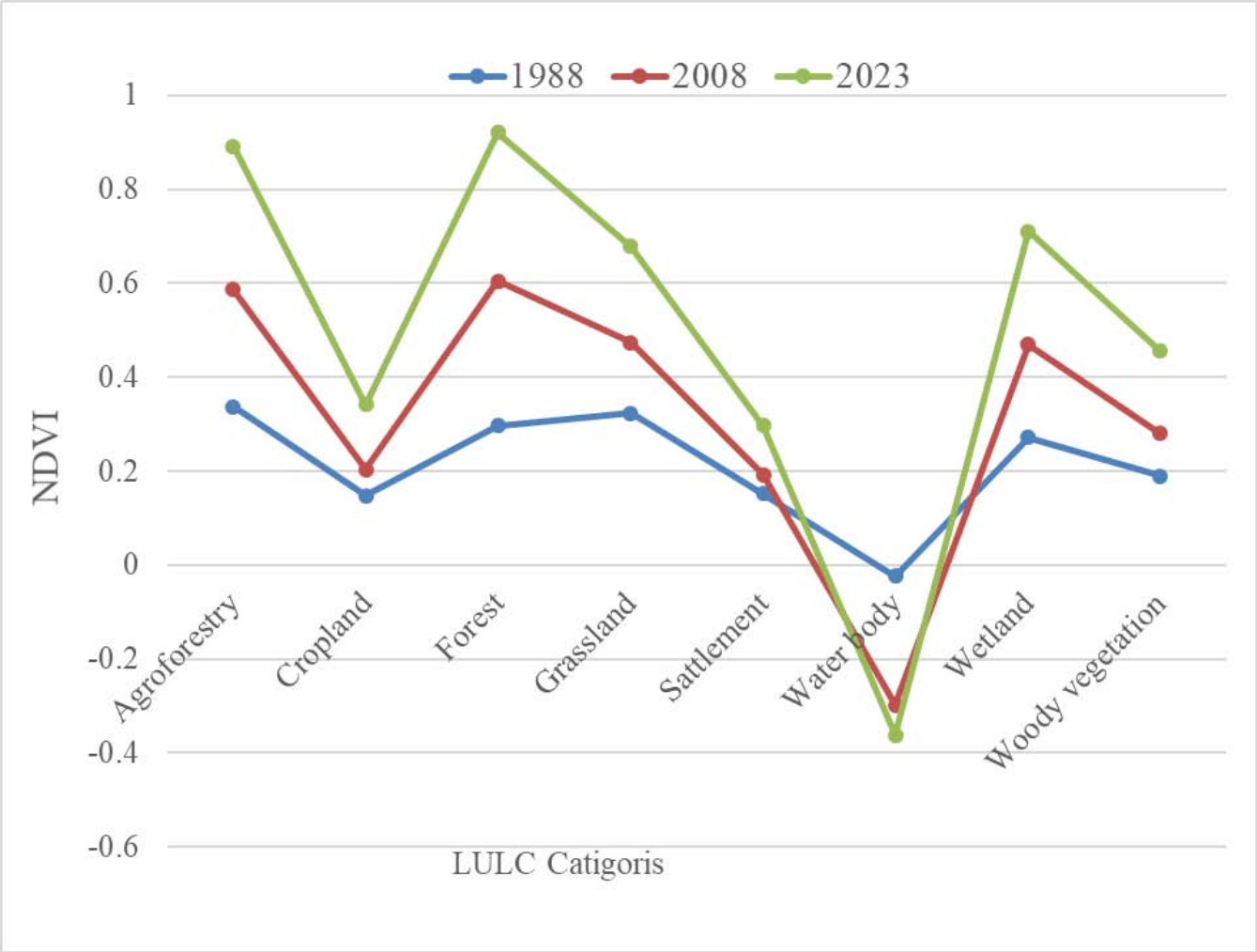

Figure.4.6.Zonal statistical description of NDVI in 1988, 2008 and2023

4.8. Relationship between LU/LC and NDBI

The NDBI maps, obtained from the short-wave infrared and near-infrared bands of the research periods, reveal variations in NDBI values across different land covers. During the dry season, cropland exhibits higher NDBI values due to its comparable reflectance and built-up short-wave infrared. Conversely, forest areas have higher reflectance in the near-infrared range but lower reflectance in the shortwave infrared spectrum. This is because the dense vegetation absorbs short-wave infrared radiation while strongly reflecting near-infrared light. The same pattern

holds true for water bodies. Figure 18 illustrates the zonal statistical description of NDBI values for the years 1988, 2008, and 2023.

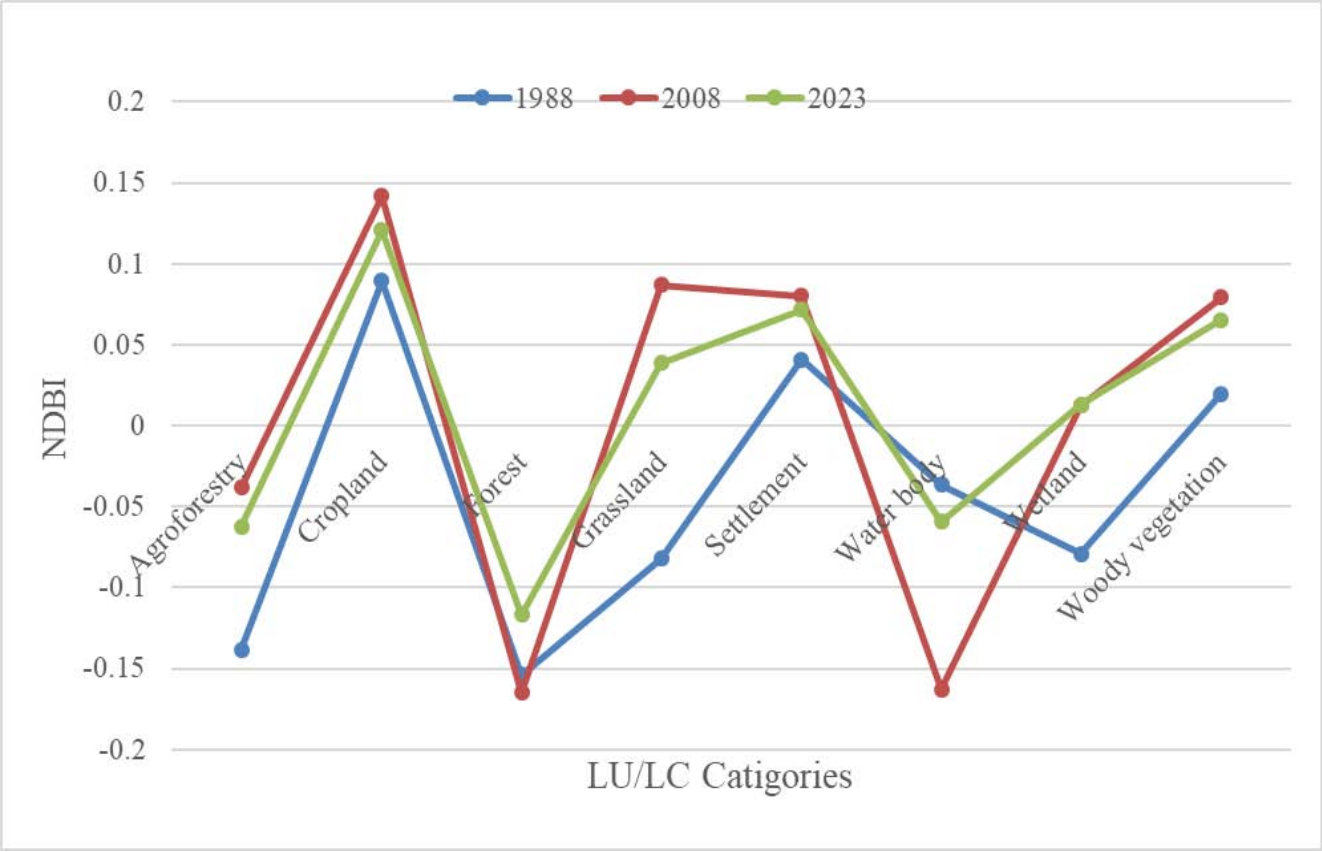

Figure.4.7. Zonal statistical description of NDBI in 1988, 2008 and 2023

4.9. Spatial-Temporal Distribution of LST in the Hawassa area

By utilizing Landsat TM images from 1988, ETM+ images from 2008, and TIRS images from 2023, we were able to retrieve and quantify the geographical distribution of LST in the research area. Through analysis of these images, we determined that the LST in the research area ranged from 12 °C to 46 °C between 1988 and 2023.The analyzed thermal pictures reveal that the research area's western and northern regions have comparatively high temperatures. The majority of those places were used for agriculture, but during the dry season, there were also some patches of bare rock that were open to the sun. On the other hand, the core regions of the LST values inside the watershed, which include Lake Hawassa and Cheleleka Wetland, were comparatively lower. Low land surface temperatures were observed in the eastern and southeast regions of the research area. This was because these areas were covered with plantation and natural forests.

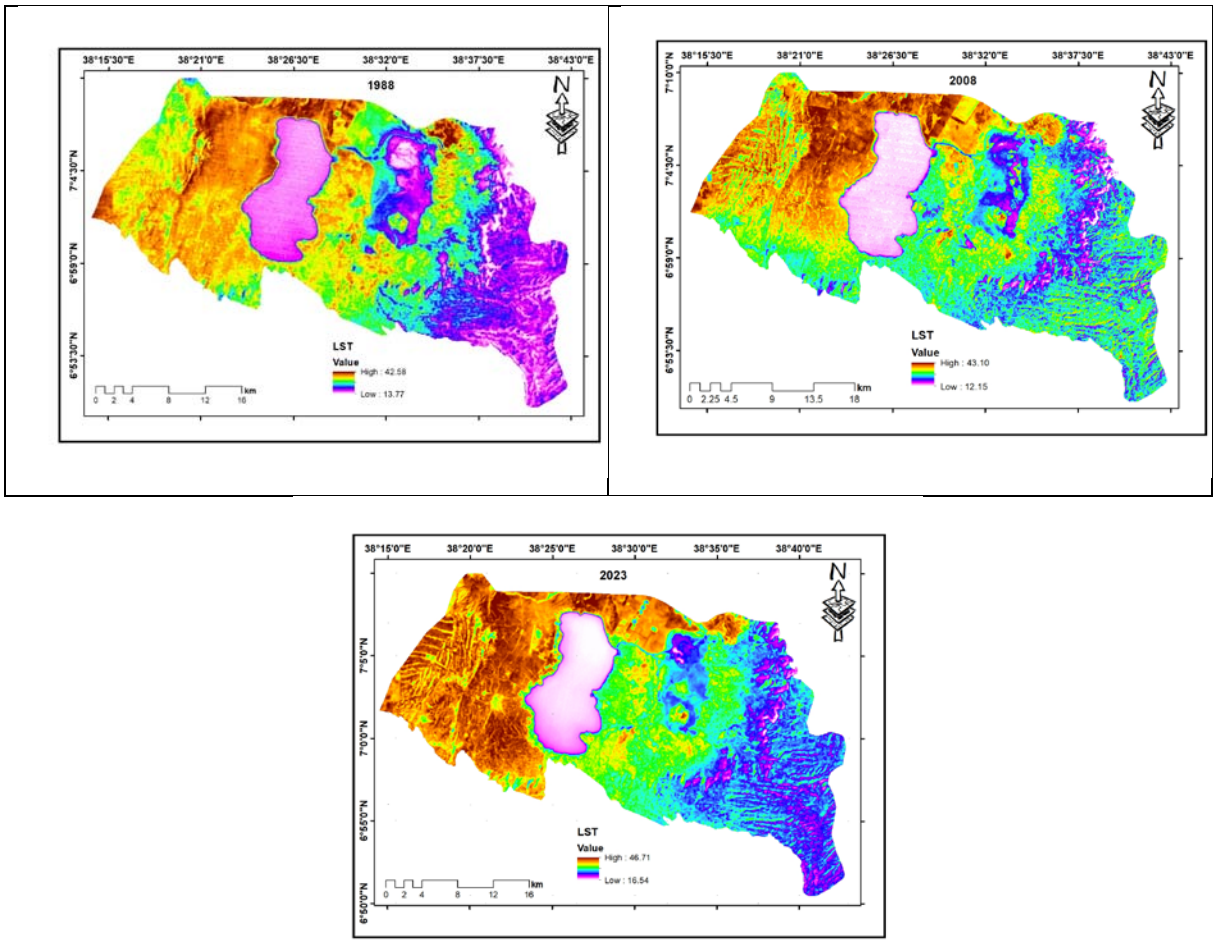

Figure.4.8. LST map of the study area for the years 1988, 2008 and2023

4.10. The Impacts of LU/LC Change on Land Surface Temperature

Changes in land use and land cover, particularly in areas with towns, harvested crops, and barren ground, directly affect the temperature of the Earth's surface. As a result, there are variations in land surface temperature.Because the research was done using an image taken during the harvest season and in dry weather, elevated land surface temperatures were seen in agriculture areas.

It is important to note that variations in vegetation and climate conditions lead to changes in land surface temperature among different land use and land cover groups. In contrast, forests have a lower reflectance in the shortwave infrared spectrum and a higher reflectance in the near-infrared region. The conversion of various land uses into residential zones has resulted in an increase in land surface temperature. Figure 14 illustrates the significant growth of Hawassa City from 1988 to 2023, with the northern, southern, and western parts of the city experiencing the most

substantial growth. Additionally, the smaller towns in the Hawassa area have also witnessed a population increase.

Table.4.6. A zonal statistical depiction of LST over various LU/LC in 1988, 2008, and 2023

		1988				2008			2023			
class name	MIN	MAX	MEAN	STD	MIN	MAX	MEAN	STD	MIN	MAX	MEAN	STD
Agroforestry	16.10	37.61	22.37	2.49	14.92	35.92	25.63	2.42	18.66	39.51	26.15	2.01
Cropland	17.93	42.59	33.80	2.78	18.15	43.11	33.87	3.90	19.34	46.58	37.94	4.58
Forest	13.78	29.18	19.48	1.99	12.16	28.82	20.38	2.48	16.55	32.99	23.92	2.30
Grassland	18.38	38.39	25.11	3.19	19.74	40.46	29.66	2.44	19.54	45.56	30.87	5.86
Settlement	21.50	42.59	33.32	2.92	13.82	41.35	29.76	4.08	19.75	45.96	33.18	3.13
Water body	14.25	29.18	19.91	0.71	16.55	35.46	17.82	0.81	16.75	33.61	18.95	1.08
Wetland	16.10	41.07	24.93	3.41	17.09	40.90	26.36	3.51	18.59	45.21	30.69	4.52
Woody vegetation	15.64	41.83	30.85	4.88	14.37	41.79	29.52	4.42	18.46	46.71	34.10	5.37

WHERE, MIN=MINMUM, MAX = MAXIMUM AND STD = STANDARDDEVATION

More than 30.42% of the study area was used for agriculture during the investigation period. Additionally, the land surface temperature (LST) has shown an upward trend over time. In 1988, the average LST was 33.97°C, while in 2023, it had risen to 37.94°C.

4.11. The relationship between LU/LCLST

The map of LU/LC and LST in the study area showed the changes in categories during the study period, along with the corresponding temperatures.The LU/LC categories with the lowest recorded temperatures were agroforestry, forest, and water bodies. Lowering LST is achieved when both vegetation and bodies of water are present. The process of evapotranspiration, which involves plants releasing water into the atmosphere, is a contributing factor. The abundance of trees and vegetated areas in the area creates shade, which helps to decrease air and land surface temperatures. Conversely, cropland and settlements exhibit the highest LST values. Throughout the duration of the image collection, the LST values in cropland remained consistently high. In fact, from 1988 to 2023, the average LST in the Hawassa area increased by 3.97°C.The regions with the highest average LST were found in densely populated areas and cropland. On the other hand, the lowest average LST was observed in agroforestry zones, forestland, and water bodies.

Figure 4.10 illustrates the comparison of mean LST values with different LU/LC classes throughout the study period.

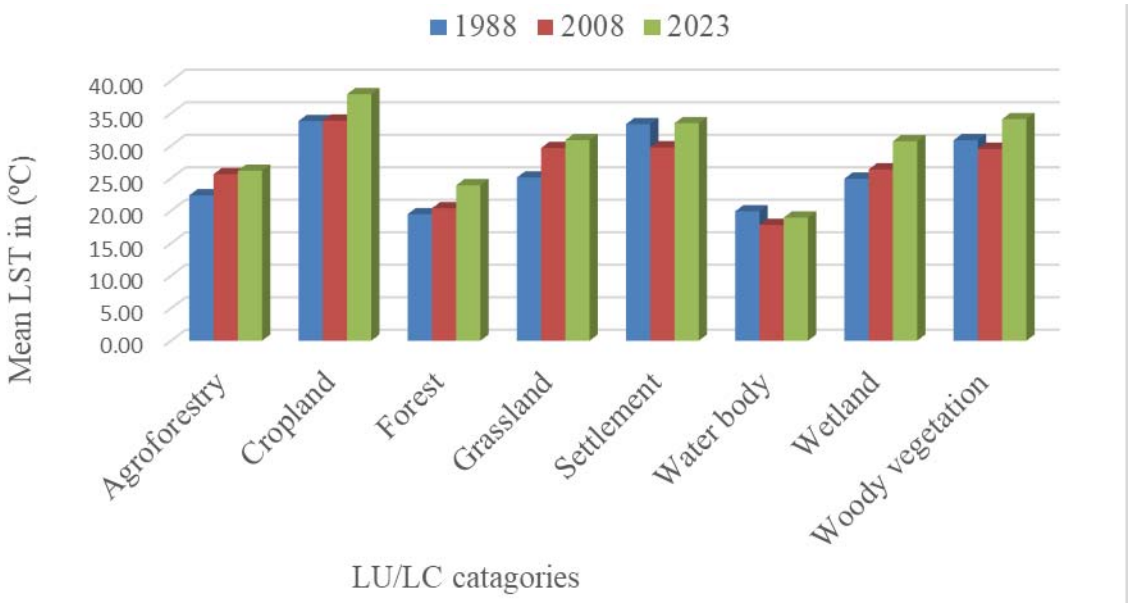

Figure.4.9. mean LST in each land cover class's in1988, 2008 and 2023

4.12. Correlation Between NDVI and LST for the study period

The range of NDVI values varies from a maximum of 0.55 to a minimum of -0.37, whereas the range of LST values extends from the maximum temperature of 46.70°C to the minimum temperature of 12.16°C. The analysis of Landsat images from 1988, 2008, and 2023 revealed indirect correlations between NDVI and LST, as shown in Figure 21. This suggests that land cover classes with lower NDVI values tend to have higher LST values. In other words, there is a negative correlation between the NDVI value and the radiant surface temperature value for each type of land cover.According to Ullah et al. (2023), the geographic distribution pattern produced by LST and NDVI values was opposite. In land cover with heavy vegetation, the NDVI value is highest and the LST is lowest, and vice versa. Additionally, the figure below demonstrates the substantial negative association between the three study years (1988, 2008, and 2023) and the NDVI. R^2 values are, in order, 0.9332, 0.9288, and 0.9431.

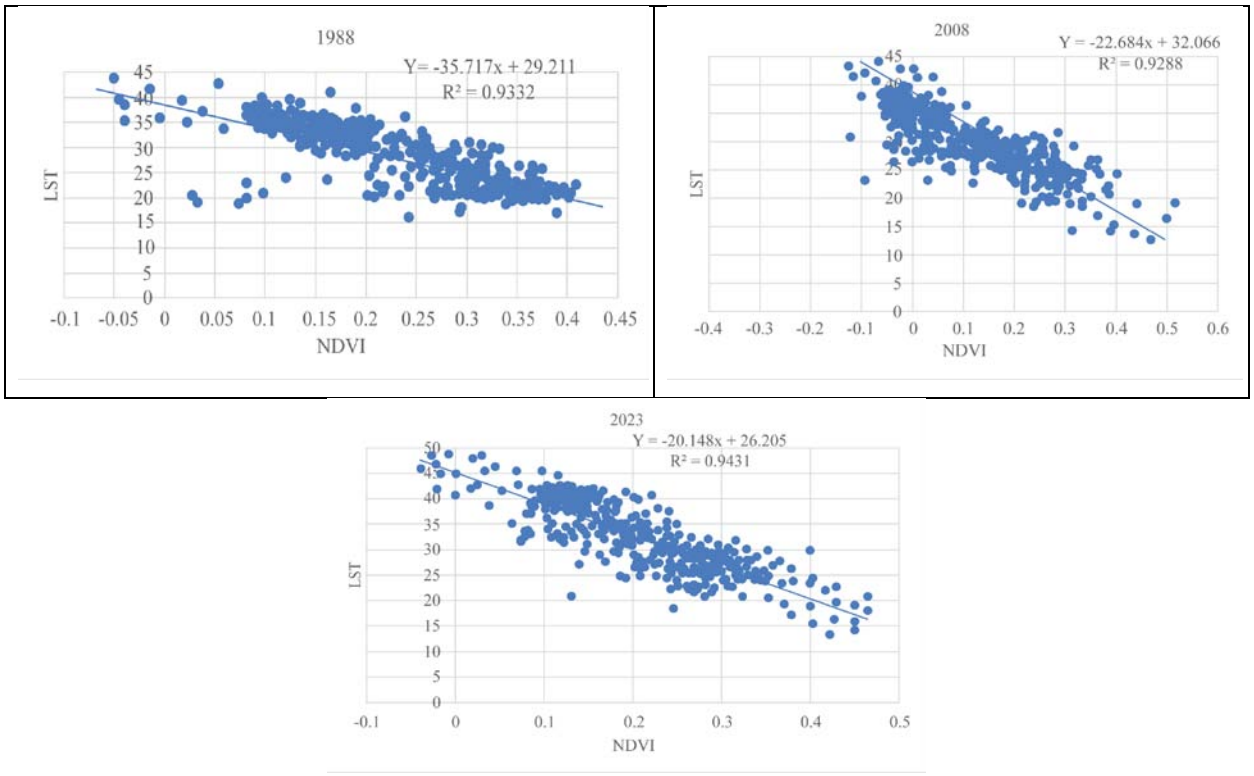

Figure.4.10. NDVI and LST correlation for the year 1988, 2008 and 2023

4.13. Correlation between NDBI and LST during the study period

The study found a direct link between NDBI and LST, which was observed in every season. NDBI results showed that built-up regions had the highest LST. This led to the hypothesis that urbanization and built-up areas are responsible for significant fluctuations in land surface temperature. The years 1988, 2008, and 2023 showed a significant positive association between NDBI and LST (R^2 = 0.9908, R^2 = 0.995, and R^2 = 0.9771, respectively). This positive correlation suggests that changes in land surface temperature and urban heat islands are primarily caused by built-up regions. Figure 22 illustrates the correlation between land surface temperature and NDBI for the years 1988, 2008, and 2023.

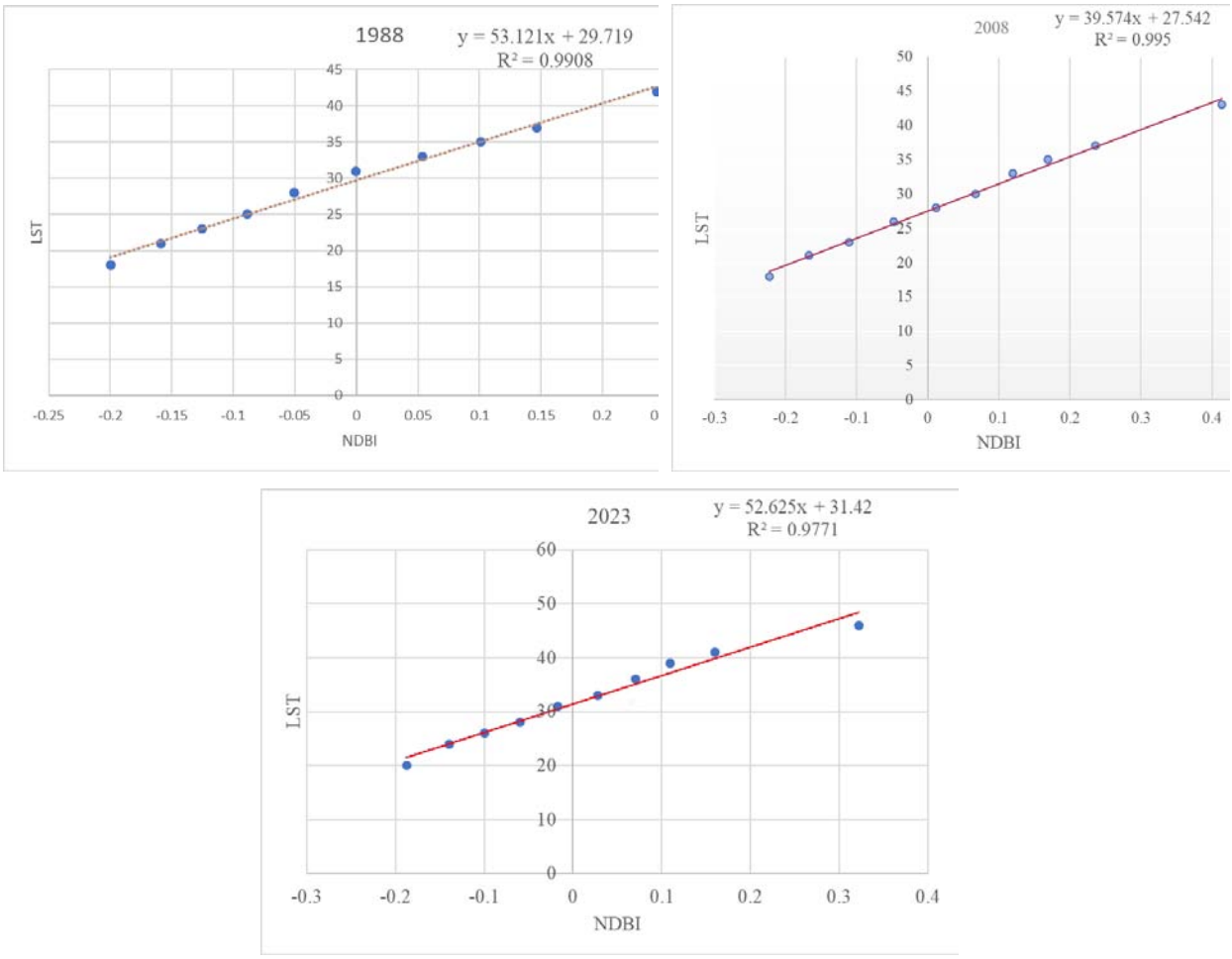

Figure.4.11.NDBI and LST correlation for the year 1988, 2008 and 2023

4.14. Comparisons of LST distribution between 1988, 2008 and 2023

The results of the study show that there has been a rise in the land surface temperature (LST) from 1988 to 2023. Throughout the study period, the LST in the study area varied between 12.15ºC and 46.71ºC. The researchers classified the land surface temperature into six categories.

Table 4.7.LST categories and their area coverage from 1988, 2008 and2023

Area in (km^2)			
LST	1988	2008	2023
<22	217.04	129.18	110.59
23 - 26	173.12	209.89	281.86
27 - 31	142.88	283.91	217.32
32 - 34	219.21	207.43	142.86

>35	274.62	196.41	274.24

4.15. Verification of Land Surface Temperature

A direct correlation has been observed between the interpolated atmospheric temperature and the land surface temperature extracted from the Landsat thermal band in the research region. The Landsat imagery used in this study was obtained during the dry weather and harvesting season, which helped determine the trend in LST. By considering the climatic conditions and time information available from Landsat, the spatial distribution of LST was confirmed. Temperature interpolations were conducted using meteorological data collected from seven stations, two located outside and five within the study area.

The two nearest stations to the research region are Leku and Shashemene. These stations were previously known as Hawassa Tabour, Tula, Hogiso, Shamena, and Wondo Genet. There is a strong correlation between the LST and the atmospheric temperature extrapolated from these stations. The interpolated map of the research area shows that the eastern region has the lowest temperature results, while the western and northwest regions have higher values. In fact, the western section consistently had the highest values during each research period, while the eastern section had lower values, as indicated by the LST results obtained from the Landsat thermal bands.

The interpolated map of the research area reveals that the temperature was lowest in the eastern region. In comparison, the west and northwest had higher temperature values. Specifically, the western portion consistently had the highest temperature value throughout each research period, while the eastern section had a lower value. These findings are based on the retrieval of Landsat thermal bands and the resulting LST values. The mean LST varied between 20.40 ºC and 34.7 ºC during the research period. In contrast, the interpolated mean atmospheric temperature ranged between 25 and 30 degrees Celsius. The following map illustrates the interpolated atmospheric temperature values.

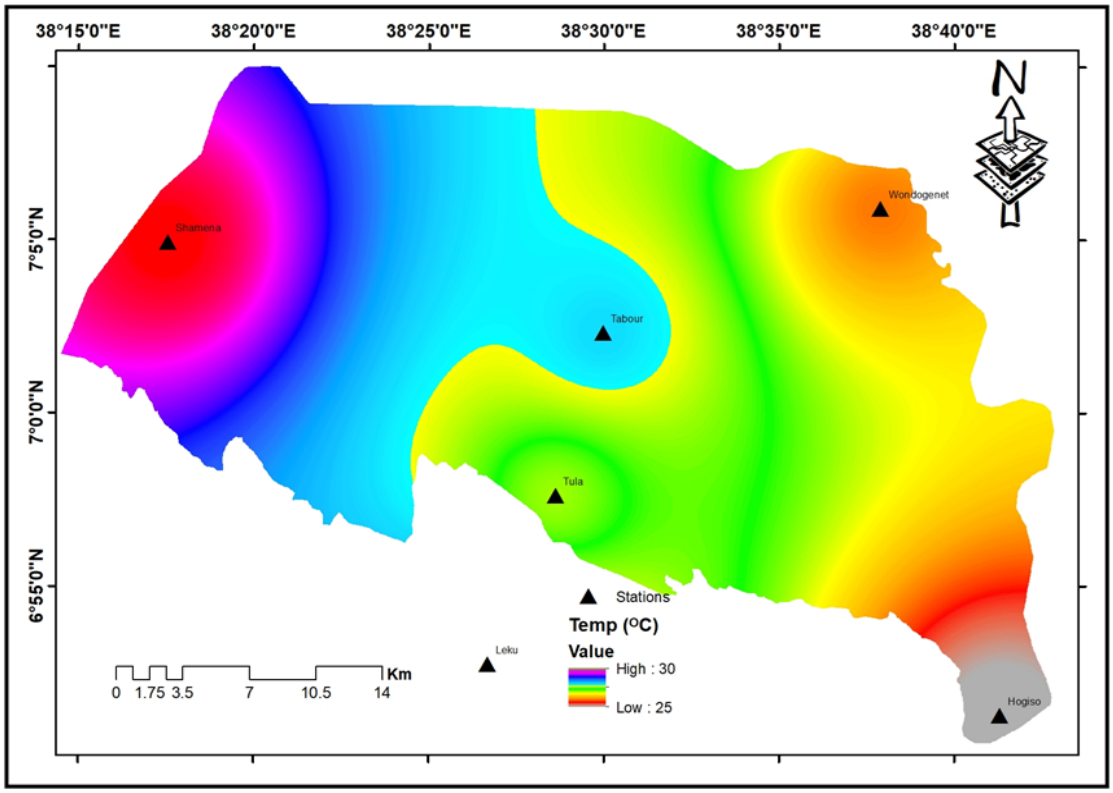

Figure.4.12. interpolated temperature map in the study area

4.16. LU/LC status in the Hawassa area

The changes in land cover and usage in the Hawassa area indicate a significant population expansion and increased demand for land for agriculture and housing. These changes have several detrimental effects on the environment. As previously mentioned,(Boserup et al., 2024).The main causes of LU/LC fluctuation in third-world countries are the increasing human population, economic progress, technological advancements, and environmental changes. Our investigation revealed significant alterations in LU/LC during the study period. The settlement area expanded from 26.04 km^2 in 1988 to 51.48 km^2 in 2023, highlighting the growing demand for settlements.Furthermore, there has been an expansion in the wetland area, increasing from 92.07 km^2 in 1988 to 114 km2 in 2023. Similarly, the grassland area has also grown, reaching 88.73 km^2 in 2023 compared to 59 km^2 in 1988. On the other hand, there have been declines in cropland and water bodies. In terms of agroforestry and woody vegetation, there is variability.

The forest area has increased to 30 km^2 in 2023 from 22.87 km^2 in 1988. These changes in land use and land cover can be observed in the classified satellite image.

4.17. Normalized difference vegetation index

NDVI is a reliable measure used to determine the condition of vegetation and LST, as noted by(Sara Afrasiabi et al., 2013). Their study found that NDVI can be used as a reliable indicator of dryness and LST. Additionally, their investigation revealed that the NDVI values varied from east to west across the studied area. This region is predominantly comprised of land classes such as woody vegetation, agroforestry, and farmland, resulting in a diverse range of vegetation covers.The study determined that the correlation coefficient between the NDVI and LST for the year 2023 was $R^2 = 0.9431$. This indicates that the vegetation state has a significant impact on the local LST, with the NDVI accounting for 94.31% of the LST distribution. Thus, the study found a strong correlation between NDVI and LST, except in the case of the water body class.

4.18. Normalized difference built up index

This confirms the well-known predictions that built-up regions significantly contribute to the increase in LST. This association has been confirmed by several authors, including(Nse et al., 2020), (Das & Angadi, 2021), (Guha et al., 2018), and (Obiefuna et al., 2021).The NDBI results show a strong positive correlation with the indices for 1988, 2008, and 2023 ($R^2 = 0.9908$), as well as for 2008 ($R^2 = 0.995$) and 2023 ($R^2 = 0.9771$). This indicates that the NDBI results have a similar tendency to the LST. In contrast to impermeable surfaces such as built-up and bare land regions, vegetated and wetland areas exhibit lower LST. This suggests a higher rate of evapotranspiration and promotes latent exchange between the surface and the atmosphere.(Alademomi et al., 2020).

In the past two decades, studies have consistently shown that both vegetation cover and water content of the surface soil play a significant role in affecting surface radiation temperature. It has been observed that vegetated surfaces tend to experience less temperature fluctuation compared to urban surfaces. Therefore, the variations in pixel temperatures are likely to be primarily influenced by the quantity and characteristics of built-up areas. Moreover, the NDBI considers the extent of built-up areas(Macarof & Statescu, 2017).

4.19. Land surface temperature

Based on our research, it has been determined that areas with cropland and settlements (built-up regions) experience the highest land surface temperatures.Similar findings were discovered by researchers in theZhejiang Delta,China by (Weng, 2010)and in Metu, southwest Ethiopia by (Megersa et al., 2023).These studies aimed to assess the relationship between LU/LC and thermal signatures.The primary reason for the low NDVI and high LST values in the cropland LU/LC class is that the image was taken in February and March, which coincides with the dry season in Ethiopia. These months are crucial for harvesting, and as a result, both the cropland and settlement classes showed significant surface reflectivity. After the crops were harvested, the soil became extremely dry and highly reflective.

The NDVI values are generally lower for cropland, settlement, and water bodies. However, they are relatively higher for woody vegetation and agroforestry. It is essential to establish the connection between LU/LC types and LST in order to assess the thermal condition of the land surface using satellite data. The Normalized Difference Vegetation Index plays a significant role in evaluating and researching LST. Except for water bodies, there are indirect correlations between LST and NDVI across different LU/LC categories.Similar findings were observed by(Fan et al., 2020)Similar findings were observed by Fan et al. (2020) in their evaluation of Compositing the Minimum NDVI for Daily Water Surface Mapping in Poyang Lake, China. This is because water has poor reflectance in both NIR and red wavelengths, resulting in negative or nearly zero NDVI values. Consequently, water bodies in the LU/LC class exhibit low NDVI and LST values. It should be noted that the NDVI value of vegetation and the type of LU/LC do have an impact on the LST value, but they are not the sole factors contributing to its increase. Other factors such as soil types, geothermal energy, elevation, geological context, and local climate conditions can also influence the LST value.

Both (Gashaw et al., 2014) and(Karbalaee et al., 2023)agree that the primary causes of the increase in LST in both rural and urban areas are changes in land cover and uncontrolled use of land resources. The relationship between land-cover change, biodiversity, and land degradation is particularly strong in less developed areas. Consequently, forests and other vegetation have been replaced by human settlements, croplands, and grazing grounds. In the research region, there has been a decrease in cropland due to the expansion of woody vegetation and settlements,

which can be observed in the classified satellite image of the Hawassa area. However, it is worth noting that land-use and land-cover changes can sometimes have positive effects on the environment. For instance, the gradual increase in forested areas could potentially help mitigate the rising LST in the research region.

According to (Malik et al., 2019)their study revealed a direct correlation between the NDBI and LST in each season. The NDBI results indicate that built-up regions experience higher maximum surface temperatures. This finding supports the hypothesis that urbanization and built-up areas contribute to significant fluctuations in surface temperature. Specifically, the study found a strong positive link between NDBI and LST in every season, with R^2 values of 0.9908 in 1988, 0.995 in 2008, and 0.9771 in 2023.

The positive correlation between NDBI and LST suggests that the built-up region is the main cause of LST changes and urban heat islands. Conversely, a dense vegetation canopy is crucial for reducing surface temperature. The study's findings reveal eight main LU/LC classes, each with different LST values. Agroforestry, forests, and water bodies have relatively low LST. Wetlands have a moderate LST value, while crops, urban settlements, and grasslands with woody vegetation have high LST values. The spatial and temporal distribution of LST in 1988, 2008, and 2023 demonstrates changes that occurred in the region over the study period. In 1988, the distribution of LST ranged from 13.77ºC to 42ºC, with a minimum and maximum, respectively. In 2008 and 2023, the minimum and maximum LST ranges were 12.15ºC–43.0ºC and 16.54ºC–46.71ºC, respectively.

CHAPTR FIVE

5. CONCLUSION AND RECOMMENDATIONS

5.1. Conclusion

Persistent and undesired changes in land cover often serve as the primary drivers of environmental changes across various spatial scales. These changes can have detrimental impacts, such as the disruption of climate patterns that are closely linked to LST. In this study, we utilized GIS and remote sensing tools to investigate the dynamics of land cover and its influence on land surface temperature in the Hawassa area of Ethiopia's central rift valley.

The study aimed to understand the impact of changes in land cover on the spatial-temporal distribution and variations in LST. To achieve this, data from Sentine-2A, Landsat 5 TM, Landsat 7 ETM+, and Landsat 8 TIRS were utilized. Satellite images have proven to be invaluable in monitoring and analyzing changes in land cover, vegetation, and ecosystems, providing valuable insights into the environmental implications.

In the Hawassa area, eight distinct land cover classes were identified using the physical features' characteristics. The LU/LC pattern in the study area has been linked to the socioeconomic and environmental factors, as well as their spatial and temporal utilization. The study's results revealed significant changes in the land cover of the study locations over the past 35 years.From 1988 to 2023, there was consistent growth in settlement, forest, grassland, and wetland areas. However, cropland and water bodies experienced a consistent decrease throughout the research period, while agroforestry and woody vegetation showed fluctuations.

In the research area, there have been regular changes in land use and cover. The minimum and maximum LST have increased each year. Consequently, the calculated LST has an impact on local temperature and significantly affects LU/LC functions. The study's findings indicate that LSTs in the Hawassa area have increased from 1988 to 2023. Furthermore, the LST values obtained from satellite data align well with the estimated temperature values from the weather stations used in this study.

5.2. Recommendations

The study focused on using satellite imagery to evaluate how changes in land cover affect the distribution and spatial-temporal variability in land surface temperature in the Hawassa area. According to this study, one of the main causes of the periodic and location-specific increases in LST was the changing of land cover. As a result, the recommendations that follow are derived from the study's findings.

- Land cover change has become a vital aspect of current resource management and environmental change monitoring strategies. As a result, it is crucial for governmental and non-governmental agencies to prioritize both proper land use management and the ecological impact of each land cover. This is supported by the thesis results for example the trained of water bodies continuously decrease the all over the study year.
- It is crucial to practice integrated environmental management, which includes preserving the current plant cover, managing land uses appropriately, reforesting steep slopes, and raising local community knowledge.
- Even if LCC is a significant element for variance in LST, it is crucial to look into additional aspects like topography and elevation.
- Find a way to maintain a balance between the growing population and the limited natural resources.
- In this study, we only analyzed Landsat and Sentiel-2A images taken during the dry season for LST analysis. However, it is worth considering that multi-season and daylight and night temperature difference satellite data could be beneficial for future researcher.

Reference

Abir, F. A., & Saha, R. (2021). Assessment of land surface temperature and land cover variability during winter: A spatio-temporal analysis of Pabna municipality in Bangladesh. *Environmental Challenges*, *4*(April). https://doi.org/10.1016/j.envc.2021.100167

Addo, K. A. (2010). Urban and peri-urban agriculture in developing countries studied using remote sensing and in situ methods. *Remote Sensing*, *2*(2), 497–513. https://doi.org/10.3390/rs2020497

Ahmed, B., Kamruzzaman, M. D., Zhu, X., Shahinoor Rahman, M. D., & Choi, K. (2013). Simulating land cover changes and their impacts on land surface temperature in dhaka, bangladesh. *Remote Sensing*, *5*(11), 5969–5998. https://doi.org/10.3390/rs5115969

Aires, F., Prigent, C., Rossow, W. B., & Rothstein, M. (2001). A new neural network approach including first guess for retrieval of atmospheric water vapor, cloud liquid water path, surface temperature, and emissivities over land from satellite microwave observations. *Journal of Geophysical Research Atmospheres*, *106*(D14), 14887–14907. https://doi.org/10.1029/2001JD900085

Al-doski, J., Mansor, S. B., Zulhaidi, H., & Shafri, M. (2013). Image Classification in Remote Sensing. *Journal of Environment and Earth Science*, *3*(10), 141–148.

Alademomi, A. S., Okolie, C. J., Daramola, O. E., Agboola, R. O., & Salami, T. J. (2020). Assessing the relationship of LST, NDVI and EVI with land cover changes in the Lagos Lagoon environment. *Quaestiones Geographicae*, *39*(3), 87–109. https://doi.org/10.2478/quageo-2020-0025

Anand, A. (2018a). Accuracy Assessment. *ResearchGate*, *January 2017*, 59–77. https://www.researchgate.net/publication/319963167_PROCESSING_AND_CLASSIFICATION_OF_REMOTELY_SENSED_IMAGES

Anand, A. (2018b). Unit 13 Image Classification. *ResearchGate*, *January 2017*, 41–55.

Ashima Kalra, Dr. Aiyah S. Noori, M. V. and M. J. N. (2022). Digital Image Processing. In *AGPH Books (Academic Guru Publishing House)* (First edit, Issue April). AGPH Books (Academic Guru Publishing House). https://doi.org/10.1016/B978-012170960-0/50064-5

Awad, M., & Khanna, R. (2015). Support Vector Machines for Classification. *Resaearc Gete*, *April 2015*, 1–248. https://doi.org/10.1007/978-1-4302-5990-9

Azad O. Rasul. (2016). Remote Sensing of Surface Urban Cool and Heat Island Dynamics in Erbil, Iraq, between 1992 and 2013. *University of Leicester*.

Bankman, I. N. (2009). Handbook of Medical Image Processing and Analysis. In I. N. BANKMAN (Ed.), *Academic Press* (Second Edi, Vol. 34, Issue 7, pp. 535–538). https://doi.org/10.1016/B978-0-12-373904-9.50007-6

Becker, F., & Zhao-Liang Li. (1995). Surface temperature and emissivity at various scales: definition, measurement and related problems. *Remote Sensing Reviews*, *12*(3–4), 225–253.

https://doi.org/10.1080/02757259509532286

Belete, F., Maryo, M., & Teka, A. (2023). Land use/land cover dynamics and perception of the local communities in Bita district, south western Ethiopia. *International Journal of River Basin Management*, *21*(2), 211–222. https://doi.org/10.1080/15715124.2021.1938092

Berihun, M. L., Tsunekawa, A., Haregeweyn, N., Meshesha, D. T., Adgo, E., Tsubo, M., Masunaga, T., Fenta, A. A., Sultan, D., & Yibeltal, M. (2019). Exploring land use/land cover changes, drivers and their implications in contrasting agro-ecological environments of Ethiopia. *Land Use Policy*, *87*(May), 104052. https://doi.org/10.1016/j.landusepol.2019.104052

Betts, A. K., Ball, J. H., Beljaars, A. C. M., Miller, M. J., & Viterbo, P. A. (1996). The land surface-atmosphere interaction: A review based on observational and global modeling perspectives. *Journal of Geophysical Research Atmospheres*, *101*(D3), 7209–7225. https://doi.org/10.1029/95JD02135

Bhardwaj, N., Kaur, G., & Singh, P. K. (2018). A systematic review on image enhancement techniques. *Advances in Intelligent Systems and Computing*, *651*(April), 227–235. https://doi.org/10.1007/978-981-10-6614-6_23

Boserup, E., Population, S., Review, D., & Mar, N. (2024). Environment, Population, and Technology in Primitive Societies. *JSTOR*, *2*(1), 21–36.

Buermann, W., Wang, Y., Dong, J., Zhou, L., Zeng, X., Dickinson, R. E., Potter, C. S., & Myneni, R. B. (2002). Analysis of a multiyear global vegetation leaf area index data set. *Journal of Geophysical Research Atmospheres*, *107*(22), ACL 14-1-ACL 14-16. https://doi.org/10.1029/2001JD000975

Campbell, D. J., Lusch, D. P., Smucker, T. A., & Wangui, E. E. (2005). Multiple methods in the study of driving forces of land use and land cover change: A case study of SE Kajiado District, Kenya. *Human Ecology*, *33*(6), 763–794. https://doi.org/10.1007/s10745-005-8210-y

Campbell, J., & Shin, M. E. (2011). Essentials of GIS. *Saylor.Org*, 24.

Chaudhary, B. S., Saroha, G. P., & Yadav, M. (2008). Human Induced Land Use/Land Cover Changes in Northern Part of Gurgaon District, Haryana, India: Natural Resources Census Concept. *Journal of Human Ecology*, *23*(3), 243–252. https://doi.org/10.1080/09709274.2008.11906077

Chayapong, P., & Dasananda, S. (2012). Analysis of urban heat island phenomenon and its relationships with land use/land cover characteristics: Case study in Bangkok metropolitan administration area. *33rd Asian Conference on Remote Sensing 2012, ACRS 2012*, *2*, 989–995.

Chen, X. (2002). Using remote sensing and GIS to analyse land cover change and its impacts on regional sustainable development. *International Journal of Remote Sensing*, *23*(1), 107–124. https://doi.org/10.1080/01431160010007051

Coppin, P., Jonckheere, I., Nackaerts, K., Muys, B., & Lambin, E. (2004). Digital change detection methods in ecosystem monitoring: A review. *International Journal of Remote Sensing*, *25*(9), 1565–1596. https://doi.org/10.1080/0143116031000101675

Das, S., & Angadi, D. P. (2021). Land use land cover change detection and monitoring of urban growth using remote sensing and GIS techniques: a micro-level study. *GeoJournal*, *87*(3), 2101–2123. https://doi.org/10.1007/s10708-020-10359-1

Debie, E., Anteneh, M., & Asmare, T. (2022). Land Use/Cover Changes and Surface Temperature Dynamics Over Abaminus Watershed, Northwest Ethiopia. *Air, Soil and Water Research*, *15*, 2–16. https://doi.org/10.1177/11786221221097917

Deribew, K. T., & Dalacho, D. W. (2019). Land use and forest cover dynamics in the North-eastern Addis Ababa, central highlands of Ethiopia. *Environmental Systems Research*, *8*(1), 1–18. https://doi.org/10.1186/s40068-019-0137-1

Eastman, J. (2009). IDRISI Taiga: Guide to GIS and Image Processing Volume - Manual version 16.02. *Clark University*, *August*, 182–185.

Elias, E., Seifu, W., Tesfaye, B., & Girmay, W. (2019). Impact of land use/cover changes on lake ecosystem of Ethiopia central rift valley. *Cogent Food and Agriculture*, *5*(1), 1–20. https://doi.org/10.1080/23311932.2019.1595876

Emad H.E. Yasin, C. K. (2023). Evaluating Satellite Image Classification: Exploring Methods and Techniques. *Intechopen*, *11*(tourism), 13. https://www.intechopen.com/books/advanced-biometric-technologies/liveness-detection-in-biometrics

Fan, X., Liu, Y., Wu, G., & Zhao, X. (2020). Compositing the minimum NDVI for daily water surface mapping. *Remote Sensing*, *12*(4). https://doi.org/10.3390/rs12040700

FAO. (2010). *Global Forest resource assessment. Forestery Paper 163, Rome, Italy*.

FAO. (2016). Forests and agriculture: land-use challenges and opportunities. In *State of the World's Forests* (Vol. 45, Issue 12). http://ccafs.cgiar.org/news/press-releases/agriculture-and-food-production-contribute-29-percent-global-greenhouse-gas

FAO. (2020). *Rome*, *2020*.

Galati, S. R. (2006). *Geographic Information Systems Demystified*. McGraw-Hill Education.

Gashaw, T., Bantider, A., & Mahari, A. (2014). Evaluations of Land Use/Land Cover Changes and Land Degradation in Dera District, Ethiopia: GIS and Remote Sensing Based Analysis. *International Journal of Scientific Research in Environmental Sciences*, *2*(6), 199–208. https://doi.org/10.12983/ijsres-2014-p0199-0208

Gebrelibanos, T., & Assen, M. (2015). Land use/land cover dynamics and their driving forces in the Hirmi watershed and its adjacent agro-ecosystem, highlands of Northern Ethiopia. *Journal of Land Use Science*, *10*(1), 81–94. https://doi.org/10.1080/1747423X.2013.845614

Gebreslassie, H. (2014). Land Use-Land Cover dynamics of Huluka watershed, Central Rift Valley, Ethiopia. *International Soil and Water Conservation Research*, *2*(4), 25–33. https://doi.org/10.1016/S2095-6339(15)30055-1

Geist, H. J., & Lambin, E. F. (2002). Proximate causes and underlying driving forces of tropical deforestation. *BioScience*, *52*(2), 143–150. https://doi.org/10.1641/0006-3568(2002)052[0143:PCAUDF]2.0.CO;2

Geist, H., McConnell, W., Lambin, E. F., Moran, E., Alves, D., & Rudel, T. (2006). Land-Use and Land-Cover Change. In *Land-Use and Land-Cover Change*. https://doi.org/10.1007/3-540-32202-7_3

Georgakis, C., & Santamouris, M. (2017). Determination of the surface and canopy urban heat island in Athens central zone using advanced monitoring. *Climate*, *5*(4). https://doi.org/10.3390/cli5040097

Getahun, S., & Yoseph, M. (2022). Land use land cover changes and its implication on ecotourism in hawassa city and its surroundings'. *Ukrainian Journal of Ecology*, *12*(2), 19–25. http://glovis.usgs.gov/

Goward, S. N., Tucker, C. J., & Dye, D. G. (1985). North American vegetation patterns observed with the NOAA-7 advanced very high resolution radiometer. *NASA Publications*, 2–14.

Grinblat, Y., Kidron, G. J., Karnieli, A., & Benenson, I. (2015). Simulating land-use degradation in West Africa with the ALADYN model. *Journal of Arid Environments*, *112*(PA), 52–63. https://doi.org/10.1016/j.jaridenv.2014.05.019

Guha, S., Govil, H., Dey, A., & Gill, N. (2018). Analytical study of land surface temperature with NDVI and NDBI using Landsat 8 OLI and TIRS data in Florence and Naples city, Italy. *European Journal of Remote Sensing*, *51*(1), 667–678. https://doi.org/10.1080/22797254.2018.1474494

Halder, B., Haghbin, M., & Farooque, A. A. (2021). An Assessment of Urban Expansion Impacts on Land Transformation of Rajpur-Sonarpur Municipality. *Knowledge-Based Engineering and Sciences*, *2*(3), 34–53. https://doi.org/10.51526/kbes.2021.2.3.34-53

Hall, F. G., Huemmrich, K. F., Goetz, S. J., Sellers, P. J., & Nickeson, J. E. (1992). Satellite remote sensing of surface energy balance: success, failures, and unresolved issues in FIFE. *Journal of Geophysical Research*, *97*(D17). https://doi.org/10.1029/92jd02189

Hicke, J. A., Asner, G. P., Randerson, J. T., Tucker, C., Los, S., Birdsey, R., Jenkins, J. C., & Field, C. (2002). Trends in North American net primary productivity derived from satellite observations, 1982-1998. *Global Biogeochemical Cycles*, *16*(2), 2-1-2–14. https://doi.org/10.1029/2001gb001550

Hidalgo-García, D., & Arco-Díaz, J. (2022). Modeling the Surface Urban Heat Island (SUHI) to study of its relationship with variations in the thermal field and with the indices of land use in the metropolitan area of Granada (Spain). *Sustainable Cities and Society*, *87*(May). https://doi.org/10.1016/j.scs.2022.104166

Huang, K., Li, X., Liu, X., & Seto, K. C. (2019). Projecting global urban land expansion and heat island intensification through 2050. *Environmental Research Letters*, *14*(11). https://doi.org/10.1088/1748-9326/ab4b71

Igun, E., & Williams, M. (2018). Impact of urban land cover change on land surface temperature. *Global Journal of Environmental Science and Management*, *4*(1), 47–58. https://doi.org/10.22034/gjesm.2018.04.01.005

Jensen, J. R. (2007). *Re m ot e Se n sin g of Ve g ge t a t ion*.

Karbalaee, A. R., Hedjazizadeh, Z., & Masoodian, S. A. (2023). Dependency of LSA and LST to topographic factors in Iran, based on remote sensing data. *Theoretical and Applied Climatology*, *153*(1–2), 709–726. https://doi.org/10.1007/s00704-023-04489-y

Kumar, T. D. (2018). *REMOTE SENSING & GIS Prepared by*.

Lambin, E. F., Geist, H. J., & Lepers, E. (2003). Dynamics of land-use and land-cover change in tropical regions. *Annual Review of Environment and Resources*, *28*, 205–241. https://doi.org/10.1146/annurev.energy.28.050302.105459

Lambin, E. F., Turner, B. L., Geist, H. J., Agbola, S. B., Angelsen, A., Bruce, J. W., Coomes, O. T., Dirzo, R., Fischer, G., Folke, C., George, P. S., Homewood, K., Imbernon, J., Leemans, R., Li, X., Moran, E. F., Mortimore, M., Ramakrishnan, P. S., Richards, J. F., … Xu, J. (2001). The causes of land-use and land-cover change: Moving beyond the myths. *Global Environmental Change*, *11*(4), 261–269. https://doi.org/10.1016/S0959-3780(01)00007-3

Liu, K., Ke, T., Tao, P., He, J., Xi, K., & Yang, K. (2020). Robust Radiometric Normalization of Multitemporal Satellite Images Via Block Adjustment without Master Images. *IEEE Journal of Selected Topics in Applied Earth Observations and Remote Sensing*, *13*, 6029–6043. https://doi.org/10.1109/JSTARS.2020.3028062

Liu, L., & Zhang, Y. (2011). Urban heat island analysis using the landsat TM data and ASTER Data: A case study in Hong Kong. *Remote Sensing*, *3*(7), 1535–1552. https://doi.org/10.3390/rs3071535

Macarof, P., & Statescu, F. (2017). Comparasion of NDBI and NDVI as Indicators of Surface Urban Heat Island Effect in Landsat 8 Imagery: A Case Study of Iasi. *Present Environment and Sustainable Development*, *11*(2), 141–150. https://doi.org/10.1515/pesd-2017-0032

Malik, M. S., Shukla, J. P., & Mishra, S. (2019). Relationship of LST, NDBI and NDVI using landsat-8 data in Kandaihimmat watershed, Hoshangabad, India. *Indian Journal of Geo-Marine Sciences*, *48*(1), 25–31.

Marchant, R., Richer, S., Boles, O., Capitani, C., Courtney-Mustaphi, C. J., Lane, P., Prendergast, M. E., Stump, D., De Cort, G., Kaplan, J. O., Phelps, L., Kay, A., Olago, D., Petek, N., Platts, P. J., Punwong, P., Widgren, M., Wynne-Jones, S., Ferro-Vázquez, C., … Wright, D. (2018). Drivers and trajectories of land cover change in East Africa: Human and environmental interactions from 6000 years ago to present. *Earth-Science Reviews*, *178*(August 2017), 322–378. https://doi.org/10.1016/j.earscirev.2017.12.010

Margareth, H. (2017). ENVIRONMENTAL PROTECTION and FOREST DEVELOPMENT AROUND HAWASSA CITY AND THE LAKE. *Czech Aid*, 5.

Mariye, M., Jianhua, L., Maryo, M., Tsegaye, G., & Aletaye, E. (2024). Remote sensing and GIS-based study of land use/cover dynamics, driving factors, and implications in southern Ethiopia, with special reference to the Legabora watershed. *Heliyon*, *10*(1), e23380. https://doi.org/10.1016/j.heliyon.2023.e23380

Mather, A. S., & Needle, C. L. (2000). The relationships of population and forest trends. *Geographical Journal*, *166*(1), 2–13. https://doi.org/10.1111/j.1475-4959.2000.tb00002.x

Megersa, W., Deribew, K. T., Abreha, G., Liqa, T., Moisa, M. B., Hailu, S., & Worku, K. (2023). Stochastic modeling of urban growth using the CA-Markov chain and multi-scenario prospects in the tropical humid region of Ethiopia: Mettu. *Geocarto International*, *38*(1). https://doi.org/10.1080/10106049.2023.2240285

Mehmood, M., Shahzad, A., Zafar, B., Shabbir, A., & Ali, N. (2022). Remote Sensing Image Classification: A Comprehensive Review and Applications. *Mathematical Problems in Engineering*, *2022*. https://doi.org/10.1155/2022/5880959

Mitchell, A. L., Rosenqvist, A., & Mora, B. (2017). Current remote sensing approaches to monitoring forest degradation in support of countries measurement, reporting and verification (MRV) systems for REDD+. *Carbon Balance and Management*, *12*(1). https://doi.org/10.1186/s13021-017-0078-9

Moisa, M. B., Busha Hinkosa, L., Negasa, G. F., Olika, G., Ijigu, T. E., Wedajo, Y. N., Gurmessa, M. M., Deribew, K. T., & Gemeda, D. O. (2023). GIS and remote sensing Based Analysis of Land use and Land cover Change in the Upper Anger watershed, Western Ethiopia. *Geology, Ecology, and Landscapes*, *00*(00), 1–10. https://doi.org/10.1080/24749508.2023.2237323

Muhati, G. L., Olago, D., & Olaka, L. (2018). Land use and land cover changes in a sub-humid Montane forest in an arid setting: A case study of the Marsabit forest reserve in northern Kenya. *Global Ecology and Conservation*, *16*(2018), e00512. https://doi.org/10.1016/j.gecco.2018.e00512

Myneni , Hall , Sellers, M. (1995). The Interprtation of Spectral Vegetation Indexes. *TRANSACTIONS ON GEOSCIENCE AND REMOTE SENSING*, *33*, 1–6.

Myneni, R. B., Keeling, C. D., Tucker, C. J., Asrar, G., & Nemani, R. R. (1997). Increased plant growth in the northern high latitudes from 1981 to 1991. *Nature*, *386*(6626), 698–702. https://doi.org/10.1038/386698a0

Negassa, M. D., Mallie, D. T., & Gemeda, D. O. (2020). Forest cover change detection using Geographic Information Systems and remote sensing techniques: a spatio-temporal study on Komto Protected forest priority area, East Wollega Zone, Ethiopia. *Environmental Systems Research*, *9*(1), 1–14. https://doi.org/10.1186/s40068-020-0163-z

Nse, O. U., Okolie, C. J., & Nse, V. O. (2020). Dynamics of land cover, land surface temperature

and NDVI in Uyo City, Nigeria. *Scientific African*, *10*, e00599. https://doi.org/10.1016/j.sciaf.2020.e00599

Nzoiwu, C. P., Agulue, E. I., Mbah, S., & Igboanugo, C. P. (2017). Impact of Land Use/Land Cover Change on Surface Temperature Condition of Awka Town, Nigeria. *Journal of Geographic Information System*, *09*(06), 763–776. https://doi.org/10.4236/jgis.2017.96047

Obiefuna, J. N., Okolie, C. J., Nwilo, P. C., Daramola, O. E., & Isiofia, L. C. (2021). Potential Influence of Urban Sprawl and Changing Land Surface Temperature on Outdoor Thermal Comfort in Lagos State, Nigeria. *Quaestiones Geographicae*, *40*(1), 5–23. https://doi.org/10.2478/quageo-2021-0001

Ojima, D. S., Galvin, K. A., & Turner, B. L. I. I. (1994). The global impact of land-use change. *BioScience*, *44*(5), 300–304. https://doi.org/10.2307/1312379

Osgouei, P. E., Kaya, S., Sertel, E., & Alganci, U. (2019). Separating built-up areas from bare land in mediterranean cities using Sentinel-2A imagery. *MDPI Remote Sensing*, *11*(3), 1–24. https://doi.org/10.3390/rs11030345

Pal, S., & Ziaul, S. (2017). Detection of land use and land cover change and land surface temperature in English Bazar urban centre. *Egyptian Journal of Remote Sensing and Space Science*, *20*(1), 125–145. https://doi.org/10.1016/j.ejrs.2016.11.003

Patón, D. (2020). Normalized Difference Vegetation Index Determination in Urban Areas by Full-Spectrum Photography. *MDPI Ecologies*, *1*(1), 22–35. https://doi.org/10.3390/ecologies1010004

Pettorelli, N., Gaillard, J. M., Mysterud, A., Duncan, P., Stenseth, N. C., Delorme, D., Van Laere, G., Toïgo, C., & Klein, F. (2006). Using a proxy of plant productivity (NDVI) to find key periods for animal performance: The case of roe deer. *Oikos*, *112*(3), 565–572. https://doi.org/10.1111/j.0030-1299.2006.14447.x

Phan, T. N., Kappas, M., & Tran, T. P. (2018). Land surface temperature variation due to changes in elevation in Northwest Vietnam. *Climate*, *6*(2), 1–19. https://doi.org/10.3390/cli6020028

Pongratz, J., Reick, C. H., Raddatz, T., & Claussen, M. (2010). Biogeophysical versus biogeochemical climate response to historical anthropogenic land cover change. *Geophysical Research Letters*, *37*(8), 1–5. https://doi.org/10.1029/2010GL043010

Potapov, P., Hansen, M. C., Kommareddy, I., Kommareddy, A., Turubanova, S., Pickens, A., Adusei, B., Tyukavina, A., & Ying, Q. (2020). Landsat analysis ready data for global land cover and land cover change mapping. *Remote Sensing*, *12*(3). https://doi.org/10.3390/rs12030426

Prince, S. D., Becker-Reshef, I., & Rishmawi, K. (2009). Detection and mapping of long-term land degradation using local net production scaling: Application to Zimbabwe. *Remote Sensing of Environment*, *113*(5), 1046–1057. https://doi.org/10.1016/j.rse.2009.01.016

Purwanto, Utomo, D. H., & Kurniawan, B. R. (2016). Spatio Temporal Analysis Trend of Land

Use and Land Cover Change Against Temperature Based on Remote Sensing Data in Malang City. *Procedia - Social and Behavioral Sciences*, *227*(November 2015), 232–238. https://doi.org/10.1016/j.sbspro.2016.06.066

Rajeshwari.A, M. . (2014). Estimation of Land Surface Temperature of Dindigul District Using Landsat 8 Data. *International Journal of Research in Engineering and Technology*, *03*(05), 122–126. https://doi.org/10.15623/ijret.2014.0305025

Ranagalage, M., Gunarathna, M. H. J. P., Surasinghe, T. D., Dissanayake, D., Simwanda, M., Murayama, Y., Morimoto, T., Phiri, D., Nyirenda, V. R., Premakantha, K. T., & Sathurusinghe, A. (2020). Multi-decadal forest-cover dynamics in the tropical realm: Past trends and policy insights for forest conservation in Dry Zone of Sri Lanka. *Forests*, *11*(8), 1–24. https://doi.org/10.3390/F11080836

Rashed, A. A. M., Atta, M., & Ahmed, O. (2021). Image Enhancement for Performance Improvement : Mathematics , Machine Learning and Deep Learning Solutions. *IEEE Access*, 1–14.

Robinson, N. P., Allred, B. W., Jones, M. O., Moreno, A., Kimball, J. S., Naugle, D. E., Erickson, T. A., & Richardson, A. D. (2017). A dynamic landsat derived normalized difference vegetation index (NDVI) product for the conterminous United States. *MDPI Remote Sensing*, *9*(8), 1–14. https://doi.org/10.3390/rs9080863

Rogan, J., & Chen, D. M. (2004). Remote sensing technology for mapping and monitoring land-cover and land-use change. *Elseiver Ltd*, *61*(4), 301–325. https://doi.org/10.1016/S0305-9006(03)00066-7

Rogan, J., & Miller, J. (2006). Integrating GIS and Remotely Sensed Data for Mapping Forest Disturbance and Change. In *Understanding Forest Disturbance and Spatial Pattern* (Issue May). https://doi.org/10.1201/9781420005189.ch6

Rouse, Haas, Schell, D. (1974). MONITORING VEGETATION SYSTEMS IN THE GREAT PLAINS WITH ERTS. *Journal of Agricultural and Food Chemistry*, *24*(1), 24–26. https://doi.org/10.1021/jf60203a024

Roy, P., & Roy, A. (2010). Land Use and Land Cover Change: A Remote Sensing & GIS Perspective. *Journal of the Indian Institute of Science*, *90*(May), 489–502.

Rozenstein, O., Qin, Z., Derimian, Y., & Karnieli, A. (2014). Derivation of Land Surface Temperature for Landsat-8 TIRS Using a Split Window Algorithm. *MDPI Open Access Sensor*, 5768–5780. https://doi.org/10.3390/s140405768

S D A P S A, & NATIONAL REMOTE SENSING CENTRE. (2014). Normalized Difference Vegetation Index(NDVI) Products by Using OCM2-GAC Sensor Data. *NATIONAL REMOTE SENSING CENTRE*, 2–5.

Sahana, M., Ahmed, R., & Sajjad, H. (2016). Analyzing land surface temperature distribution in response to land use/land cover change using split window algorithm and spectral radiance model in Sundarban Biosphere Reserve, India. *Springer International Publishing*

Switzerland, *2*(2), 1–11. https://doi.org/10.1007/s40808-016-0135-5

Salimi Kouchi, H., Sahebi, M. R., Abkar, A. A., & Valadan Zoej, M. J. (2013). Fractional Vegetation Cover Estimation In Urban Environments. *The International Archives of the Photogrammetry, Remote Sensing and Spatial Information Sciences*, *XL-1/W3*(October), 357–360. https://doi.org/10.5194/isprsarchives-xl-1-w3-357-2013

Santamouris, M. (2013). Using cool pavements as a mitigation strategy to fight urban heat island - A review of the actual developments. *Renewable and Sustainable Energy Reviews*, *26*, 224–240. https://doi.org/10.1016/j.rser.2013.05.047

Sara Afrasiabi, G., Mahdi, P., & Fatemeh, R. (2013). The Relationship between NDVI and LST in the urban area of Mashhad, Iran. *International Conference on Civil Engineering Architecture & Urban Sustainable Development*, *November*. https://www.researchgate.net/publication/265601825_The_Relationship_between_NDVI_and_LST_in_the_urban_area_of_Mashhad_Iran

Sathya, P., & Baby-Deepa, V. (2017). Analysis of Supervised Image Classification Method for Satellite Images. *International Journal of Computer Science Research (IJCSR)*, *5*(2), 16–19.

Sattari, F., & Hashim, M. (2014). A Breif Review of Land Surface Temperature Retrieval Methods from Thermal Satellite Sensors. *Middle-East Journal of Scientific Research*, *22*(5), 757–768. https://doi.org/10.5829/idosi.mejsr.2014.22.05.21934

Sayer, J. A., Harcourt, C. S., & Collins, N. M. (1992). The conservation atlas of tropical forests: Africa. In *Macmillan Publishers, Great Britain, Africa*. https://doi.org/10.2307/3451286

Singh, A. (1989). Review Articlel: Digital change detection techniques using remotely-sensed data. *International Journal of Remote Sensing*, *10*(6), 989–1003. https://doi.org/10.1080/01431168908903939

Sinha, S., Sharma, L. K., & Nathawat, M. S. (2015). Improved Land-use/Land-cover classification of semi-arid deciduous forest landscape using thermal remote sensing. *Egyptian Journal of Remote Sensing and Space Science*, *18*(2), 217–233. https://doi.org/10.1016/j.ejrs.2015.09.005

Song, J., Lin, T., Li, X., & Prishchepov, A. V. (2018). Mapping urban functional zones by integrating very high spatial resolution remote sensing imagery and points of interest: A case study of Xiamen, China. *Remote Sensing*, *10*(11). https://doi.org/10.3390/rs10111737

Song, Z., Yang, H., Huang, X., Yu, W., Huang, J., & Ma, M. (2021). The spatiotemporal pattern and influencing factors of land surface temperature change in China from 2003 to 2019. *International Journal of Applied Earth Observation and Geoinformation*, *104*, 102537. https://doi.org/10.1016/j.jag.2021.102537

Stewart, I. D., & Oke, T. R. (2012). Local climate zones for urban temperature studies. *Bulletin of the American Meteorological Society*, *93*(12), 1879–1900. https://doi.org/10.1175/BAMS-D-11-00019.1

Sun, D., & Pinker, R. T. (2003). Estimation of land surface temperature from a Geostationary

Operational Environmental Satellite (GOES-8). *Journal of Geophysical Research: Atmospheres*, *108*(11). https://doi.org/10.1029/2002jd002422

Sun, Y. (2008). Retrieval and Application of Land Surface Temperature. *Geo.Utexas.Edu*, *1*(1), 1–27. http://www.geo.utexas.edu/courses/387H/PAPERS/Term paper-Sun.pdf

Tefera, M. M. (2011). Land-Use/Land-Cover Dynamics in Nonno District, Central Ethiopia. *Journal of Sustainable Development in Africa (Volume*, *13*(4), 18–29. http://www.jsd-africa.com/Jsda/Vol13No4_Summer2011_B/PDF/A Carpentry Cutting Stock Problem1.pdf

Tempfli, K., Kerle, N., Huurneman, G. C., Janssen, L. L. F., Bakker, W. H., Feringa, W., Gieske, A. S. M., Gorte, B. G. H., Grabmaier, K. A., Hecker, C. A., Horn, J. A., Huurneman, G. C., Janssen, L. L. F., Kerle, N., Meer, F. D. Van Der, Parodi, G. N., Pohl, C., Reeves, C. V, Ruitenbeek, F. J. Van, … Woldai, T. (2009). Principles of Remote Sensing. In *The International Institute for Geo-Information Science and Earth Observation (ITC)*.

Tesfahunegn, G. B. (2014). Soil quality assessment strategies for evaluating soil degradation in Northern Ethiopia. *Applied and Environmental Soil Science*, *2014*, 438–448. https://doi.org/10.1155/2014/646502

The Scientific Committee. (2008). *Summary Report of the International Workshop on the retrieval and use of land surface temperature - bridging the gaps* (Issue October 2008).

Tolessa, T., Dechassa, C., Simane, B., Alamerew, B., & Kidane, M. (2020). Land use/land cover dynamics in response to various driving forces in Didessa sub-basin, Ethiopia. *GeoJournal*, *85*(3), 747–760. https://doi.org/10.1007/s10708-019-09990-4

Tzavali, A., Paravantis, J. P., Mihalakakou, G., Fotiadi, A., & Stigka, E. (2015). Urban heat island intensity: A literature review. *Fresenius Environmental Bulletin*, *24*(12B), 4537–4554.

United Nations Statistics Division. (2019). National Workshop on Environment Statistics in Namibia Windhoek, 3-5 December 2019 3. *National Workshop on Environment Statistics in Namibia*, *December 2019*, 3–5.

Veldkamp, A., & Lambin, E. F. (2001). Editorial: Predicting land-use change. *Agriculture, Ecosystems and Environment*, *85*(1–3), 1–6. https://doi.org/10.1016/S0167-8809(01)00199-2

Voogt, J. A., & Oke, T. R. (2003). Thermal remote sensing of urban climates. *Remote Sensing of Environment*, *86*(3), 370–384. https://doi.org/10.1016/S0034-4257(03)00079-8

Vujovic, S., Haddad, B., Karaky, H., Sebaibi, N., & Boutouil, M. (2021). Urban Heat Island: Causes, Consequences, and Mitigation Measures with Emphasis on Reflective and Permeable Pavements. *CivilEng*, *2*(2), 459–484. https://doi.org/10.3390/civileng2020026

Weng, Q. (2010). A remote sensing?GIS evaluation of urban expansion and its impact on surface temperature in the Zhujiang Delta, China. *International Journal of Remote Sensing*, *22*(10), 1999–2014. https://doi.org/10.1080/713860788

Woldeamlak. (2002). Land cover dynamics since the 1950s in Chemoga watershed , Blue Nile basin, Ethiopia. *Mountain Research and Development*, *22*(3), 263–269. https://doi.org/10.1659/0276-4741(2002)022[0263:LCDSTI]2.0.CO;2

Woldegebriel Tessema, M., & Girma Abebe, B. (2023). Quantification of land use/land cover dynamics and urban growth in rapidly urbanized countries: The case Hawassa city, Ethiopia. *Urban, Planning and Transport Research*, *11*(1). https://doi.org/10.1080/21650020.2023.2281989

Yengoh, G. T., Dent, D., Olsson, L., Tengberg, A. E., & Tucker III, C. J. (2014). Use of the Normalized Difference Vegetation Index (NDVI) to Assess Land Degradation at Multiple Scales. In *Lund University Center for Sustainability Studies (LUCSUS),*. http://link.springer.com/10.1007/978-3-319-24112-8

Yuan, F., & Bauer, M. E. (2007). Comparison of impervious surface area and normalized difference vegetation index as indicators of surface urban heat island effects in Landsat imagery. *Remote Sensing of Environment*, *106*(3), 375–386. https://doi.org/10.1016/j.rse.2006.09.003

Zhang, F., Tiyip, T., Kung, H., Johnson, V. C., Maimaitiyiming, M., Zhou, M., & Wang, J. (2016). Dynamics of land surface temperature (LST) in response to land use and land cover (LULC) changes in the Weigan and Kuqa river oasis, Xinjiang, China. *Arabian Journal of Geosciences*, *9*(7). https://doi.org/10.1007/s12517-016-2521-8

Zhang, Y., & Liang, S. (2018). Impacts of land cover transitions on surface temperature in China based on satellite observations. *Environmental Research Letters*, *13*(2). https://doi.org/10.1088/1748-9326/aa9e93

Zhao, Z. Q., He, B. J., Li, L. G., Wang, H. B., & Darko, A. (2017). Profile and concentric zonal analysis of relationships between land use/land cover and land surface temperature: Case study of Shenyang, China. *Energy and Buildings*, *155*, 282–295. https://doi.org/10.1016/j.enbuild.2017.09.046

Zubair, A. O. (2006). *Change detection in land use and land cover using geo-spatial methods : a case study of ilorin, Nigeria*. *131025*, 52.

Appendixes

Appendix 1: Report on the 1988 classification accuracy assessment.

TID *	ClassValue	C_1	C_2	C_3	C_4	C_5	C_6	C_7	C_8	Total	U_Accuracy	Kappa
1	C_1	41	0	0	1	0	0	0	0	42	0.97619	0
2	C_2	4	93	0	4	3	0	3	9	116	0.801724	0
3	C_3	2	0	7	0	0	0	0	1	10	0.7	0
4	C_4	0	0	0	16	0	0	0	0	16	1	0
5	C_5	0	0	0	0	10	0	0	0	10	1	0
6	C_6	0	0	0	0	0	21	4	0	25	0.84	0
7	C_7	0	0	0	1	0	0	24	0	25	0.96	0
8	C_8	0	1	0	0	0	0	0	36	37	0.972973	0
9	Total	47	94	7	22	13	21	31	46	281	0	0
10	P_Accuracy	0.87234	0.989362	1	0.727273	0.76923	1	0.774194	0.78260	0	0.882562	0
11	Kappa	0	0	0	0	0	0	0	0	0	0	0.85170

Where

C_1 =Agroforestry, C_2 = cropland, C_3 = Forest, C_4 = Grassland, C_5 = Settlement, C_6 = Water body, C_7 Wetland, C_8 = Woody vegetation.

Appendix 2: Report on the 2008 classification accuracy assessment.

TID	ClassValue	C_1	C_2	C_3	C_4	C_5	C_6	C_7	C_8	Total	U_Accurac	Kappa
1	C_1	32	0	0	0	0	0	1	0	33	0.969697	0
2	C_2	5	93	0	4	2	0	1	6	111	0.837838	0
3	C_3	1	0	8	1	0	0	0	0	10	0.8	0
4	C_4	1	1	0	19	0	0	0	1	22	0.863636	0
5	C_5	0	2	0	0	10	0	0	1	13	0.769231	0
6	C_6	0	0	0	0	0	23	2	0	25	0.92	0
7	C_7	0	1	1	0	0	0	28	1	31	0.903226	0
8	C_8	0	2	0	2	0	1	2	27	34	0.794118	0
9	Total	39	99	9	26	12	24	34	36	279	0	0
10	P_Accuracy	0.820513	0.939394	0.888889	0.730769	0.833333	0.958333	0.823529	0.75	0	0.860215	0
11	Kappa	0	0	0	0	0	0	0	0	0	0	0.82412

C_1 = Agroforestry, C_2 = cropland, C_3 = Forest, C_4 = Grassland, C_5 = Settlement, C_6 = Water body, C_7 Wetland, C_8 = Woody vegetation.

Appendix 3: Report on the 2023 classification accuracy assessment.

TID*	ClassValue	C_1	C_2	C_3	C_4	C_5	C_6	C_7	C_8	Total	U_Accuracy	Kappa
1	C_1	33	0	0	0	0	0	0	1	34	0.970588	0
2	C_2	0	77	0	0	4	0	0	2	83	0.927711	0
3	C_3	0	0	10	0	0	0	0	0	10	1	0
4	C_4	1	0	0	22	1	0	0	0	24	0.916667	0
5	C_5	0	1	0	0	12	0	1	0	14	0.857143	0
6	C_6	0	0	0	0	0	25	0	0	25	1	0
7	C_7	1	2	0	0	1	0	25	2	31	0.806452	0
8	C_8	0	2	0	0	2	0	1	51	56	0.910714	0
9	Total	35	82	10	22	20	25	27	56	277	0	0
10	P_Accuracy	0.942857	0.939024	1	1	0.6	1	0.925926	0.910714	0	0.920578	0
11	Kappa	0	0	0	0	0	0	0	0	0	0	0.90361

C_1 = Agroforestry, C_2 = cropland, C_3 = Forest, C_4 = Grassland, C_5 = Settlement, C_6 = Water body, C_7 Wetland, C_8 = Woody vegetation.

Appendix 4. map 1: Map of the locations of meteorological stations

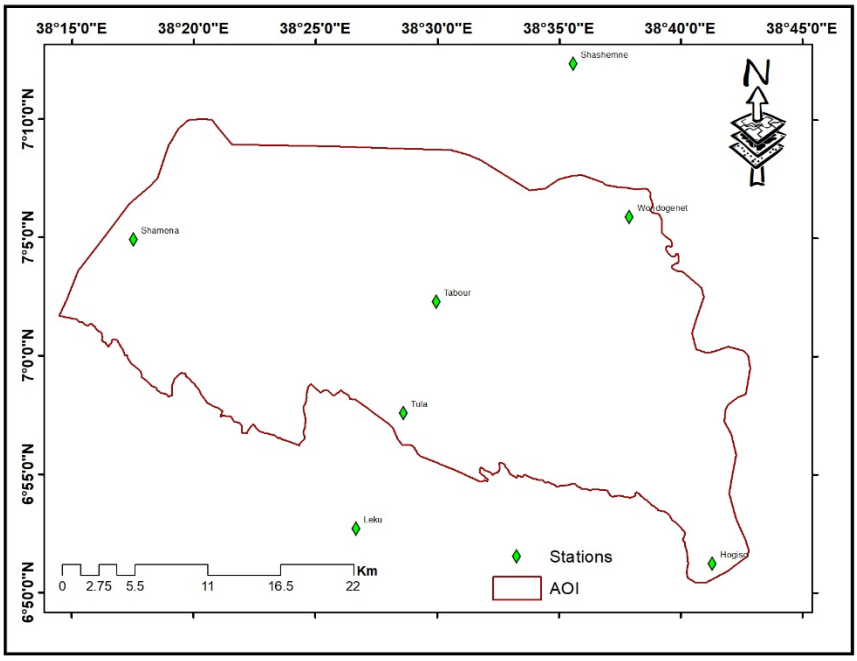

Appendix 5. map of GPS points.

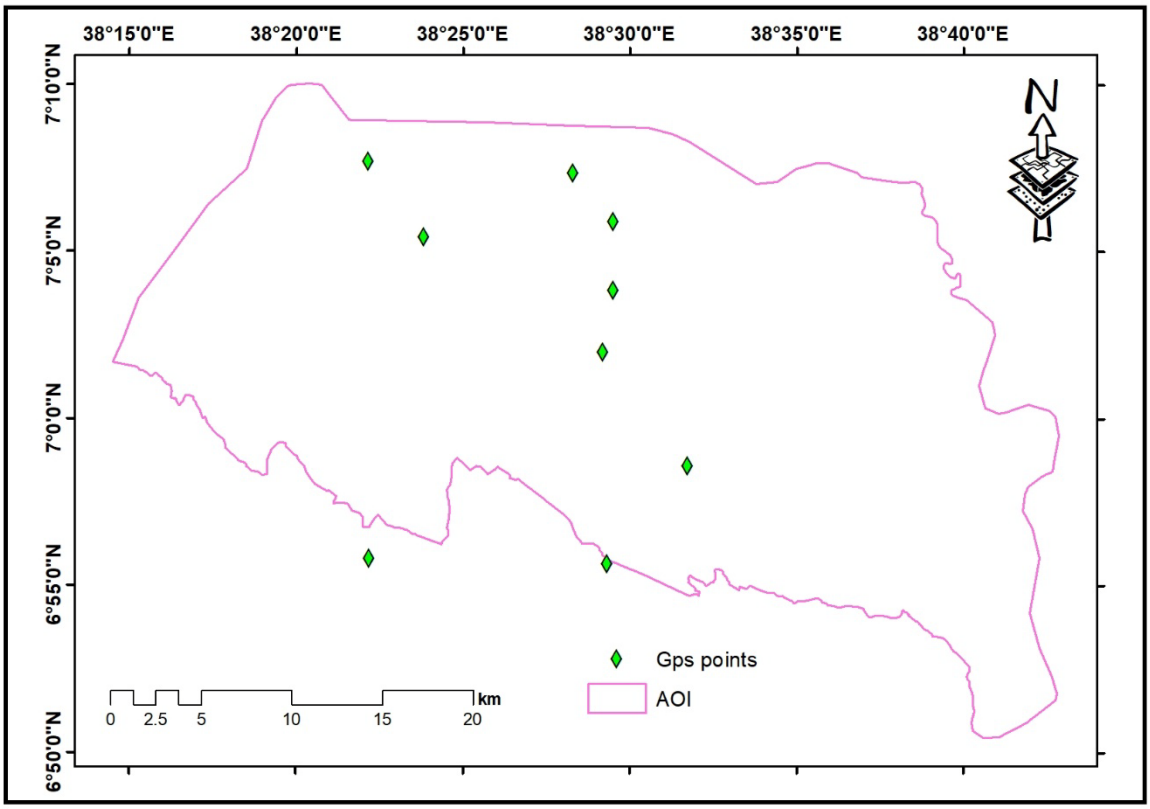

Appendix 6. An assortment of various LU/LC photos.


Forest land


Grassland


Hawass city


Hawassa lake


Wetland

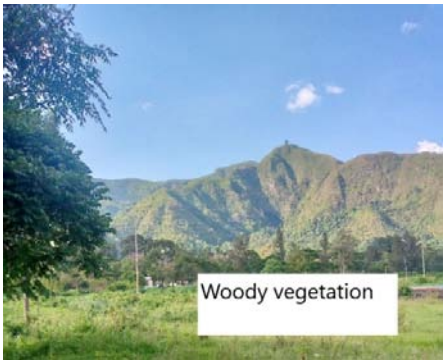
Woody vegetation


Cropland


Agroforestry

Declaration of originality

I undersigned affirm that the thesis named ASSESSING THE SPATIO TEMPORAL RELATIONSHIP BETWEEN LAND USE LAND COVER CHANGE AND LAND SURFACE TEMPERATURE CHANGE IN HAWASSA AREA, ETHIOPIA is my original work, hasn't been submitted for credit toward a degree at any other university, and has interestingly given credit to all of the sources of the materials used to create it.

Aliy Yimer Yesuf

Signature……...

Date……

Addis Ababa University

Jun,2024